THE VIBRATIONAL SPECTRA OF SOME TRIFLUOROMETHYL DERIVATIVES OF SELENIUM AND PHOSPHORUS

CENTRE FOR NEWFOUNDLAND STUDIES

TOTAL OF 10 PAGES ONLY
MAY BE XEROXED

(Without Author's Permission)

PARMOD KUMAR WAHI

c. 1

362275

CENTRE FOR NFLD. STUDIES
JUL 22 1974
MEMORIAL UNIVERSITY
OF NEWFOUNDLAND

THE VIBRATIONAL SPECTRA OF SOME TRIFLUOROMETHYL DERIVATIVES OF SELENIUM AND PHOSPHORUS

A thesis)

by

© Parmod Kumar Wahi

submitted in partial fulfillment of the requirement for the degree of Master of Science

October, 1972

Memorial University of Newfoundland

TO MY SON, KAMAL

TABLE OF CONTENTS

LIST OF TABLES

LIST OF FIGURES

ACKNOWLEDGEMENTS

I wish to express my most sincere thanks to my research supervisor, Dr. H.J. Clase, for suggesting the topic and encouragement throughout. I should also like to thank Dr. J.F. Ogilvie for the many valuable discussions during the course of this research and to my colleague and friend Mr. R.T. Pode for his many helps during the preparation of the compounds.

A fellowship and many other helps from the Chemistry Department of Memorial University of Newfoundland, and a leave of absence from the Bhabha Atomic Research Centre, Trombay, Bombay, India, are gratefully acknowledged. Special thanks are due to Dr. N.A. Narasimham, Head, Spectroscopy Division, Bhabha Atomic Research Centre, for his encouragement and getting the necessary leave sanctioned.

I owe thanks to my wife for patiently sharing with me all the hardships of a foreign graduate student. I should also like to thank Mrs. Sonia Banfield for drawing most of the figures. Thanks are also due to my friends Mrs. and Mr. Goel for their kind hospitality and inspirations without which perhaps this thesis would have taken much longer to come to the present form.

ABSTRACT

This thesis describes a detailed study of the vibrational spectra of some trifluoromethyl compounds of selenium and phosphorus: CF_3SeX (X = Cl, Br, CN, CH_3 and CF_3), $(CF_3Se)_2$, $(CF_3)_3P$, $(CF_3)_2PF$ and CF_3PF_2. The compounds were prepared by literature methods with slight modifications in some cases. Gas-phase infrared spectra were recorded in the range 4000 - 200 cm^{-1} and liquid-phase Raman spectra from 4000 - 50 cm^{-1}. Raman spectra were excited by the appropriate lines of an argon-krypton mixed gas laser. Although some vibrational wavenumbers had been previously reported for most of these compounds, there were no detailed assignments. Since this work was completed an assignment of $(CF_3)_3P$ has been published, which is somewhat in agreement with the conclusions reached here. The vibrational spectra of all these compounds have been analysed and almost all assignments made, using Raman depolarisation ratios, analogy with similar compounds and the gas-phase infrared band contour study. The infrared band contour study has proved to be very useful in confirming some of the previous assignments and making many fresh assignments. The band contour study has shown that for the molecules containing one CF_3 group, the in-plane and out-of-plane C-F stretching and CF_3

asymmetric deformation modes show a slight splitting. For the molecules containing more than one CF_3 group, the in- and out-of-phase symmetric CF_3 deformation modes are always nearly degenerate and the in-phase mode is strong in the Raman, while the out-of-phase mode is strong in the infrared. The bands corresponding to CF_3 symmetric deformation and many other modes have been found to show PQR structures. The PR separations for gas-phase infrared bands have been calculated using the recently reported method of Seth-Paul et al. The calculated PR separations show good agreement with the experimental values. As for many trifluoromethyl-phosphorus compounds studied earlier, here also the C-F symmetric stretching mode has been found to lie at higher wavenumbers than the C-F asymmetric stretching mode.

Chapter 1

INTRODUCTION

The only fluorocarbons to be reported before 1937 were carbon tetrafluoride, hexafluoroethane and tetrafluoroethylene. Later, in 1940 materials were needed for use as buffer gases, coolants, lubricants and sealants in chemical plants handling reactive uranium hexafluoride, the only uranium compound available for use in gaseous diffusion process for concentrating ^{235}U isotope required for the development of atomic bombs. The discovery that fluorocarbons are stable both chemically and thermally and inert to UF_6 led to an intensive search of methods for the synthesis of fluorocarbons. At the present time fluorocarbon analogues of many organic compounds have been prepared.

In the early 1950's, with the availability of trifluoromethyl iodide, which undergoes homolytic cleavage of the C-I bond, when either heated to 250° or exposed to ultraviolet light many perfluoromethyl derivatives of metals and non-metals were synthesized either by heating trifluoromethyl iodide and the element[1,2], or alternatively by heating a heavy metal salt of trifluoroacetic acid with the element[3,4] at high temperature. During the past two decades perfluoromethyl derivatives of almost all elements of the main groups of the periodic table have been prepared and their chemistry

compared with the corresponding methyl analogues. However, very few attempts have been made to correlate and study their vibrational spectra in detail, in spite of the fact that these compounds give very intense infrared bands in the C-F stretching region 1050-1250 cm^{-1}.

In 1954, Edgell and May[5] studied the vibrational spectra of the simple compounds CF_3I and CF_3Br and concluded that the trifluoromethyl-group behaves as a rigid group and there is a very little interaction between the internal vibrational modes of a CF_3 group and that of the framework $F_3 \equiv C\text{-}X$ (where X = I, Br). However, for CF_3CN[6] some coupling exists between the C-C stretching and the internal vibrational modes of the CF_3 group, especially the symmetric CF_3 deformation. Nabi and Sheppard[7] have studied the infrared spectra of a number of compounds containing a common trifluoromethylthio-group and found that the internal vibrational modes of this group in all these compounds could be easily assigned by comparing it with the closely related molecule CF_3Cl. Raman and infrared spectra of a large number of selenium compounds of general formulae HgX_2, $(HgX_2)Y_2^{2-}$ and XHgY (where X = CF_3Se and Y = halogen or psuedo halogen) have been studied by Clase[8] and several assignments made. He has divided the vibrational modes of these molecules into those of (a) a rigid trifluoromethyl seleno group, whose internal modes

compare very well with the closely related molecule CF_3Br, the only difference being that the lower overall symmetry of these molecules sometimes leads to the splitting of doubly degenerate modes of CF_3Br, and (b) the rigid framework HgXC or HgC_2. Thus, in general, the internal vibrations of the CF_3Se group are good group wavenumbers and do not differ much from molecule to molecule. Infrared and Raman spectra of several volatile compounds of selenium: X_2, XCl, XBr, XCN, XCH_3 and XCF_3 (where X = CF_3Se) have been studied by Bomford[9] and some assignments made.

Beg and Clark[10] (1962) seem to be the first to have studied in some detail the infrared spectra of a large number of trifluoromethyl-phosphorus compounds: CF_3PI_2, $(CF_3)_2PI$ and $(CF_3)_nPY_{3-n}$ (where Y = CH_3 or C_6H_5 and n = 1, 2 or 3). Some of their assignments although tentative appear to be wrong, in the light of later studies. In the same year, Burg and Griffiths[11] correlated the infrared spectra of a large number of trifluoromethyl derivatives of general formulae $(CF_3)_2POR$ (where R = H, D, CH_3, C_2H_5, t-C_4H_9 and $(CF_3)_2P$) and $(CF_3)_2P(O)R$ (where R = Cl, Br, CH_3 and t-C_4H_9). Subsequently Griffiths has made detailed vibrational studies on a few pentavalent trifluoromethyl-phosphorus compounds: $CF_3P(O)F_2$[12], $CF_3P(O)Cl_2$[13], CF_3PF_4[14], $(CF_3)_2PCl_3$[15] and CF_3PCl_4[16], whereas only one trivalent phosphorus compound CF_3PCl_2[17] has been studied by him. The infrared spectra of

CF_3PH_2 and CF_3PD_2 in gas and solid phases has been reported by Anthony[18]. A Ph.D thesis describing the infrared and Raman spectra of perfluoromethyl arsines: $(CF_3)_3As$, $(CF_3)_2AsCl$, $(CF_3)_2AsI$, CF_3AsCl_2 and $As_2(CF_3)_4$ has been submitted by Craft[19]. Atalla and Craig[20,21] have studied in detail the infrared spectra of difluoroamines: CH_3NF_2, CD_3NF_2 and CF_3NF_2 and made all assignments except for the torsional modes. Recently, Hendra et al.[22] have reported the vibrational spectra of $N(P(CF_3)_2)_3$.

This thesis describes the vibrational study of selenium compounds: X_2, XCH_3, XCF_3, XCl, XBr and XCN (where $X = CF_3Se$), all of which except one, XCH_3 have earlier been studied by Bomford[9], with infrared spectra recorded down to 700 cm^{-1} and a few assignments made. The present study of these compounds was undertaken and infrared spectra recorded down to 200 cm^{-1}, to review with the help of infrared band contours and other available data, the assignments already made and to make as many fresh assignments as possible. The vibrational spectra of phosphorus compounds: $(CF_3)_3P$, $(CF_3)_2PF$ and CF_3PF_2 studied here have not been earlier reported elsewhere, except for a very recent publication[23], which describes the gas phase infrared spectra, the liquid phase Raman spectra and the normal co-ordinate analysis of the compounds $P(CF_3)_3$, $As(CF_3)_3$ and $Sb(CF_3)_3$. A detailed study of the

vibrational spectra of the compounds, $(CF_3)_3P$, $(CF_3)_2PF$ and CF_3PF_2 is important, for in spite of the attached strongly electro-negative groups or atoms, the compounds, CF_3PF_2 and $(CF_3)_2PF$ have been found to be good ligands[24,25,26,27] through their strong π-accepting ability which is enhanced by the presence of electronegative groups. In one report[27], infrared and Raman spectra of complexes of the type trans $L_3Mo(CO)_3$ (where L = $(CF_3)_2PF$, CF_3PF_2, CCl_3PF_2, $ROPF_2$ etc.) have been presented. From the values of carbonyl stretching absorptions and scatterings, and using simplified Cotton-Kraihanzel force field, force constants have been calculated, which show fluorophosphines have strong π-accepting ability almost comparable to that of carbon monoxide. The following decreasing order of π-acceptor ability has been proposed: $CF_3PF_2 > (CF_3)_2PF > PF_3 > CCl_3PF_2 > ClCH_2PF > PhPF_2$ $ROPF_2 > RPFNR_2 > (R_2N)_2PF$. It is hoped that a detailed study of the vibrational spectra of these ligands will lead to a more direct understanding of the nature of bonding on complex formation and interpretation of the spectra of these complexes.

Alkyl fluorophosphines cannot be prepared by the metathetical reaction

$$R_nPCl_{3-n} + \frac{3-n}{3} SbF_3 \longrightarrow R_nPF_{3-n} + \frac{3-n}{3} SbCl_3 \qquad (i)$$

but instead the following oxidation[28,29,30] takes place

$$R_nPCl_{3-n} + \frac{5-n}{3} SbF_3 \longrightarrow R_nPF_{5-n} + \frac{3-n}{3} SbCl_3 + \frac{2}{3} Sb \qquad (ii)$$

However, fluorophosphines containing an electronegative substituent (e.g. R = CF_3, CCl_3, CH_2Cl) undergo only reaction (i) and not (ii). This is because the attached electronegative group withholds the lone pair of electrons on phosphorus from entering into oxidation. This is probably why the vibrational spectra of the corresponding methyl fluorophosphines have not been studied.

The study of vibrational spectra is useful as many times one can eliminate various possible structures of a molecule and predict the correct structure by counting the number of active fundamentals and coincidences between them in the infrared and Raman. A detailed study of vibration-rotation fine structure under favourable circumstances can give structural parameters. Also, by studying related compounds, one can make important correlations which can be fruitful in establishing the structure and interpreting the spectra of other compounds.

The assignments in the present study are mainly based on the following criteria.

(i) Study of infrared gas phase band contours.

(ii) Study of the Raman depolarization ratio (ρ), which can distinguish between the totally symmetric (ρ = 0 - 6/7) and asymmetric vibrations (ρ = 6/7).

(iii) The fact that in general symmetric vibrations are more intense in the Raman, while asymmetric vibrations are more intense in the infrared.

(iv) Comparison with the spectra of closely related molecules.

Chapter 2

THEORY

This chapter gives a brief but sufficient review of the theory on the basis of which the results in Chapter 5 will be discussed.

2.1 Vibrational Spectra

For an 'n' atomic system there are 3n - 6 or 3n - 5 vibrational degrees of freedom depending upon whether the molecule is non-linear or linear. Therefore, one needs 3n - 6 or 3n - 5 co-ordinates to describe the vibrational motions of this molecule. There are several ways to describe these co-ordinates, the most useful being the system in which each of the independent 3n - 6 or 3n - 5 co-ordinates describes the motion of the atoms in its simplest form such that all atoms move in-phase with the same frequency. This system of co-ordinates is called a normal co-ordinate and the mode associated with each normal co-ordinate is called a normal mode.

Assuming a simple harmonic motion for these atoms, the wave equation of the system can be solved quantum-mechanically and the energy levels can be expressed as a function of normal modes by the following equation

$$E(v_1, v_2 \ldots v_x) = h\nu_1(v_1 + 1/2) + h\nu_2(v_2 + 1/2) + \ldots + h\nu_x(v_x + 1/2) \qquad (1)$$

where $x = 3n - 5$ or $3n - 6$, h = Planck's constant, ν_i = frequency associated with the i'th mode, v_i = vibrational quantum number.

The energy of the vibrationless ground state is obtained by putting all $v_i = 0$, while the energy of i'th fundamental vibration is obtained by putting all v's = 0 and $v_i = 1$ in the above equation. Putting $v_i = 2$ and $v_{j\neq i} = 0$ gives the energy of the first overtone of the i'th fundamental. The energy of the combination bands is obtained by putting two or more v_i's non-zero in the equation (1). The difference bands result when the initial state is not the vibrationless ground state and the transition takes places from one level v_i to another v_k such that $v_k > v_i$, then the frequency of the transition is equal to $\nu_k - \nu_i$. The intensity of the $\nu_k - \nu_i$ band is much smaller than that of the $\nu_k + \nu_i$ band since the number of molecules in the initial stage is much smaller, corresponding to Boltzmann factor $e^{-h\nu_i/kT}$. Under the harmonic oscillator approximation only fundamentals are allowed. Overtone and combination bands become allowed only if one considers anharmonicities in the motions of the atoms. So in the first approximation overtone and combination bands are forbidden

and therefore in practice are normally weaker than fundamentals themselves.

One can determine the symmetry type of these 3n - 6 or 3n - 5 vibrations using the principals of group theory and matrix algebra, provided the symmetry of the molecule is known.

2.1.1 Selection Rules

If $_i(v_i)$ represents the wave function of the i'th mode in the v'th quantum state, then the total vibrational wave function is given by

$$_v = \psi_1(v_1).\ \psi_2(v_2).\ \psi_3(v_3)\ .....\ \psi_x(v_x) \qquad (2)$$

where x = 3n - 6 or 3n - 5

when each of v_i = zero, the molecule is in its vibrational ground state and the vibrational wave function is represented by ψ^0_v. The wave function for the i'th fundamental is obtained by putting each $v_{j \neq i} = 0$ in the equation (2) and is represented by ψ^i_v. For a fundamental transition to occur by absorption of infrared dipole radiation, it is necessary that one of the following integrals be non-zero.

$$\int \psi^0_v\, x\, \psi^i_v\, d\tau$$

$$\int \psi^0_v\, y\, \psi^i_v\, d\tau \qquad (3)$$

$$\int \psi^0_v\, z\, \psi^i_v\, d\tau$$

Therefore, a fundamental will be infrared active if the normal mode involved belongs to the same representation as any one of the three cartesian co-ordinates.

For the Raman scattering it is necessary that at least one integral of the type

$$\int \psi_v^0 \, P \, \psi_v^1 \, d \quad \text{(where } P = \text{an element of the polarizability tensor)} \qquad (4)$$

be non-zero. A fundamental transition will be Raman active if the normal mode involved belongs to the same representation as one or more components of the polarizability tensor of the molecule. Generally, P is one of the quadratic functions of cartesian co-ordinates, e.g. x^2, y^2, z^2, xy, yz, zx, $x^2 - y^2$.

2.2 Infrared Band Contours

2.2.1 Calculations of Principal Moments of Inertia and Their Directions

The moments of inertia are calculated by the method of Hirschfelder[31], using the relations

$$D = \Sigma_i m_i(y_i^2 + z_i^2) - 1/M(\Sigma_i m_i y_i)^2 - 1/M(\Sigma_i m_i z_i)^2 \quad (5)$$

$$E = \Sigma_i m_i(x_i^2 + z_i^2) - 1/M(\Sigma_i m_i x_i)^2 - 1/M(\Sigma_i m_i z_i)^2 \quad (6)$$

$$F = \Sigma_i m_i(x_i^2 + y_i^2) - 1/M(\Sigma_i m_i x_i)^2 - 1/M(\Sigma_i m_i y_i)^2 \quad (7)$$

$$G = \Sigma_i m_i x_i y_i - 1/M(\Sigma_i m_i x_i)(\Sigma_i m_i y_i) \quad (8)$$

$$H = \Sigma_i m_i x_i z_i - 1/M(\Sigma_i m_i x_i)(\Sigma_i m_i y_i) \quad (9)$$

$$I = \Sigma_i m_i y_i z_i - 1/M(\Sigma_i m_i y_i)(\Sigma_i m_i z_i) \quad (10)$$

where m_i = mass of i'th atom: x_i, y_i and z_i = cartesian co-ordinates of the i'th atom.

These formulae have the advantage that the reference framework may have its origin at any place within the molecule and the directions of the axes are arbitrary, although the three principal axes must pass through the centre of gravity of the molecule and must be mutually perpendicular. The principal values of the moments of inertia can be obtained by expanding the determinant

$$\begin{vmatrix} I-D & -G & -H \\ -G & I-E & -I \\ -H & -I & I-F \end{vmatrix} = 0 \qquad (11)$$

which gives a cubic equation on expansion. The three roots of this cubic equation are the values of principal moments of inertia and are denoted by I_{XX}, I_{YY} and I_{ZZ}. For molecules having symmetry of C_{2v} or higher, the elements G, H and I of determinant (11) are zero, provided the highest fold axis is chosen to be one of the arbitrary axis, with the results that D, E and F represent principal moments of inertia. In the case of molecules belonging to C_s symmetry (as is the case with majority of the molecules studied here) it was found that if xy denotes the plane of symmetry in these molecules, the value of F was the same as one of the roots of the cubic equation, say I_{ZZ}, but the values of the other two roots were different from D and E respectively. This is because the true directions of I_{XX} and I_{YY} (the principal inertial axes in the plane) are not the same as those of the arbitrary axes x and y. Let us assume that the true axes (X and Y) make an angle ω with the direction of the arbitrary axes and let X_i, Y_i and Z_i be the cartesian co-ordinates of the i'th atom of mass m_i in the new co-ordinate system. Then the new

co-ordinates of the i'th atom, X_i, Y_i and Z_i are related to its old co-ordinates, x_i, y_i and z_i by the relations

$$X_i = x_i\cos\omega + y_i\sin\omega \qquad (12)$$

$$Y_i = -x_i\sin\omega + y_i\cos\omega \qquad (13)$$

$$Z_i = z_i \qquad (14)$$

Now, in the new co-ordinate system

$$I_{XX} = \Sigma_i m_i(Y_i^2 + Z_i^2) - 1/M(\Sigma_i m_i Y_i)^2 - 1/M(\Sigma_i m_i Z_i)^2$$

substituting the values of X_i, Y_i and Z_i from relations (12), (13) and (14) and after rearrangement, one obtains

$$I_{XX} = \Sigma_i m_i(x_i^2 + z_i^2) - 1/M(\Sigma_i m_i x_i)^2 - 1/M(\Sigma_i m_i z_i)^2$$
$$+ \cos^2\omega\left[\left\{\Sigma_i m_i y_i^2 - 1/M(\Sigma_i m_i y_i)^2\right\}\right.$$
$$\left. - \left\{\Sigma_i m_i x_i^2 - 1/M(\Sigma_i m_i x_i)^2\right\}\right]$$
$$- 2\sin\omega\cos\omega\left[\Sigma_i m_i x_i y_i - 1/M\Sigma_i(m_i x_i)(m_i y_i)\right]$$

using relations (5), (6) and (8), one obtains

$$I_{XX} = E + \cos^2\omega\,(D - E) - 2\sin\omega\cos\omega(G)$$

or $$(D - E)\cos2\omega - 2G\sin\omega\cos\omega - I_{XX} + E = 0 \qquad (15)$$

Applying trigonometric relations $\cos^2\omega = (1 + \cos2\omega)/2$ and $2\sin\omega\cos\omega = \sin2\omega$ to equation (15), one obtains

$$(D - E)\cos2\omega - 2G\sin2\omega + D + E - 2I_{XX} = 0 \qquad (16)$$

Solution of equation (16) gives the angle ω by which the arbitrary x-axis has to be rotated to get the true I_{XX} axis.

All molecules can be divided into four broad categories (i) linear (ii) symmetric rotor (iii) asymmetric rotor (iv) spherical rotor, depending on the relative magnitudes of their rotational constants, which according to the notations recommended by the Joint Commission for Spectroscopy[32] are denoted by A, B and C, such that $A \geqslant B \geqslant C$ and are expressed in cm^{-1} (using relations $A = h/8\pi^2 cI_{XX}$ etc. where I_{XX} = least principal moment of inertia). Thus if

	$A = \infty$ and $B = C$	(linear)
	$A > B = C$	(prolate symmetric rotor)
	$A = B > C$	(oblate symmetric rotor)
	$A > B > C$	(asymmetric rotor)
and	$A = B = C$	(spherical rotor)

The following asymmetry parameters are in frequent use

$$\kappa = (2B - A - C)/(A - C) \qquad (17)$$

$$\rho^* = (A - C)/B \qquad (18)$$

$$\beta + 1 = A/B \quad \text{(prolate rotor)} \qquad (19a)$$

$$\beta + 1 = C/B \quad \text{(oblate rotor)} \qquad (19b)$$

κ can have values $-1 \leq \kappa \leq +1$

$\kappa = -1$	(prolate symmetric rotor)
$\kappa = +1$	(oblate symmetric rotor)

$0 < \kappa < -1$ (prolate asymmetric rotor)

$0 < \kappa < +1$ (oblate asymmetric rotor)

ρ^* can have values $0 \leq \rho^* \leq \infty$

$\rho^* = 0$ (spherical rotor)

$0 < \rho^* < \infty$ (prolate symmetric and asymmetric rotor)

$\rho^* > 1$ (oblate symmetric rotor)

β can have values $-1/2 \leq \beta \leq \infty$

$-1/2 < \beta < 0$ (oblate symmetric and asymmetric rotor)

$0 < \beta < \infty$ (prolate symmetric and asymmetric rotor)

$\beta = 0$ (spherical top)

2.2.2 Symmetric Rotor

The energy of a prolate symmetric rotor under harmonic oscillator and rigid rotor approximations can be written as follows

$$E = \Sigma_i h\nu_i(v_i + 1/2) + B_{(v)}J(J + 1) + (A_{(v)} - B_{(v)})K^2 \qquad (20)$$

where the dependence of rotational constant on vibrational quantum number is shown by subscript (v). In a symmetric rotor the vibrations can be divided into two classes, parallel and perpendicular, depending upon whether the dipole moment oscillates parallel or perpendicular to the highest symmetry axis, which represents for prolate and oblate symmetric rotors A and C axis respectively. The corresponding infrared

bands are termed as parallel and perpendicular respectively. The selection rules, for the parallel bands are

$$\Delta K = 0 \quad \Delta J = 0, \pm 1 \quad \text{if } K \neq 0$$

$$\Delta K = 0 \quad \Delta J = \pm 1 \quad \text{if } K = 0$$

while for the perpendicular bands, the selection rules are

$$\Delta K = \pm 1 \quad \Delta J = 0, \pm 1$$

Transition corresponding to $\Delta J = -1$, 0 and +1 give rise to P, Q and R branches of the band respectively.

For simple molecules having large rotational constants it is possible to apply equation (20) exactly and study the rotational fine structure. However, the majority of molecules of interest to the chemist have small rotational constants and it is not possible to observe the rotational fine structure, since under the experimental conditions, the width of rotational transition is more than the spacing between the rotational lines themselves. Gerhard and Dennison[33] have studied the envelopes of the infrared absorption bands for symmetric rotors and found that the band envelope is a function of two parameters (i) intensity of Q branch and (ii) the PR separation.

(a) Parallel Band

The intensity of the Q branch for a parallel band

is a function of β and is expressed as

$$R(\beta) = I_Q/L \quad . \tag{21}$$

where I_Q = intensity of Q branch alone and L = total intensity of the whole band.

$$I_Q = L\left[\log\left(\sqrt{\beta} + \sqrt{\beta+1}\right) - \sqrt{\Phi}\right]/\beta\sqrt{\Phi} \qquad \beta > 0 \tag{22}$$

$$I_Q = L\left[\sqrt{-\Phi} - \sin^{-1}\sqrt{-\beta} \;/\; (-\beta\sqrt{-\Phi})\right] \qquad \beta < 0 \tag{23}$$

where $\Phi = \beta/\beta+1$

$$I_Q = L/3 \qquad \beta = 0 \tag{24}$$

The Q branch has maximum intensity for $\beta = -1/2$. In the region $0 < \beta < -\infty$ the intensity of the Q branch decreases with increasing β, until for $\beta = \infty$ (the linear molecule) $I_Q = 0$. The PR separation is given by

$$\Delta\nu(PR) = 58(\beta)(2BT/9)^{1/2} \text{ cm}^{-1} \quad . \tag{25}$$

where $\log_{10} S(\beta) = 0.721/(\beta+4)^{1.13}$

(b) Perpendicular Band

For a perpendicular band, the R-function, equation (21), is more complex. However, the Q branch should be of comparable intensity relative to the P and R branches when $\beta \simeq -1/2$ and the PR separation is smaller than the corresponding parallel band. The intensity of the Q branch is enhanced with increasing β and is equal to 1/3 of total intensity of the whole band for $\beta = 0$ and the PR separation slightly

increases. For positive values of β, the central peak becomes broad and lower, while the doublet separation increases over that of a parallel band. For values of $\beta > 1$ the envelope no longer presents an appearance of three maxima and, for sufficiently large values of β, the envelope resembles a Guassian error curve. Gerhard and Dennison[33] have calculated, for perpendicular bands, the absorption coefficient as a function of the wavemumber ν, which is expressed in terms of the distance x from the band origin and defined according to the relation,

$$x = \frac{(\nu - \nu_0)}{2B} \sigma \qquad (26)$$

(where $\sigma = Bhc/kT$ and k = Boltzmann constant)

so that the figures are adaptable to molecules with any rotational constants and any temperature. They have drawn figures for $\beta = -1/2, -1/3, 1/2$ and 4. For these values of β, x can be estimated from these figures, whereas for other values of β an interpolation is to be performed and the value of x thus obtained is substituted in the following equation to obtain PR separation.

$$\nu(PR) = 10x(BT/9)^{1/2} \text{ cm}^{-1} \qquad (27)$$

However, Seth-Paul and Dijkstra[34] have shown x to be merely a function of β in the region $-1/2 < \beta < 3/4$ such that

$x(\perp) = 1/2S(\beta)\sqrt{2\beta+2}$. Therefore substituting in equation (27), one obtains

$$\nu(PR) = 5S(\beta)\sqrt{2\beta+2}(BT/9)^{1/2}$$

Using equations (19a and 19b), one obtains

$$\nu(PR) = 5S(\beta)\,(2\epsilon T/9)^{1/2} \qquad (28)$$

(where ϵ = A or C depending upon whether the molecule is prolate or oblate).

2.2.3 Asymmetric Rotor

The energy levels of an asymmetric rotor can be represented in the first approximation as the sum of the energies of the harmonic oscillator and rigid rotor and are given by the equation

$$E = \Sigma_i h\nu_i(v_i + 1/2) + 1/2(A + C)J(J + 1) + 1/2(A - C)E_{\tau(K)} \qquad (29)$$

The vibration-rotational spectra of an asymmetric rotor can be quite complicated, unless the molecule approaches the limiting case of either a prolate or an oblate symmetric rotor. In an asymmetric rotor the dipole moment change in a vibration may either be along one of the inertial axes or may not be along any axes, giving rise to A, B, C or hybrid type band contours. A prolate asymmetric rotor should give A$\parallel$, B$\perp$, C$\perp$ or hybrid, while an oblate rotor should give

C∥ , B⊥ and A⊥ or hybrid type band contours. Thus for an asymmetric rotor with $\kappa = -0.9$, the A∥ type bands will resemble the parallel band of a symmetric rotor, while the C⊥ type band will correspond more to the perpendicular band, but will show some of the features of a parallel band.

Hollas[35] has recently computed band envelopes for six types of large symmetric rotors, including the change in the rotational constant in going from the lower to the upper state and shown that the computed band envelopes can be usefully applied to the spectra of near symmetric rotors with $|\kappa| = 0.8 - 1$. He has also shown that compounds having small rotational constants resemble symmetric rotor molecules to a greater extent than the molecules with large rotational constants having the same degree of asymmetry. This is because of the rapid decrease in the effects of slight asymmetry as κ increases and κ has large values for molecules with small rotational constants.

Badger and Zumwalt[36] have calculated and drawn band envelopes for highly asymmetrical molecules with different combinations of asymmetry parameters $\rho^* = 1/3, 1/2, 3/4, 5/4$ and $\kappa = -1/2, 0, +1/2$. The PR separation for type A, B and C bands can be predicted by estimating x, defined in equation (26), from these figures and substituting in equation (27). This method has many restrictions. First, in many cases ρ^* and κ differ considerably from the above-mentioned

values, so that laborious interpolation is sometimes unavoidable for calculating x values and the corresponding branch separations. Second, many compounds have $\rho^* > 5/4$ which interferes with the extrapolation. Also the estimates of x values are not reproducible, which results in different prediction for the same molecule by different workers.

To overcome these difficulties and to eliminate uncertainties in determining x, Seth-Paul and Dijkstra[34] have worked out a procedure and reduced x to a number, a constant ratio or a function of constants, whose values depend on and κ and are given in Table 2[34]. However, for certain values of ρ^*, Seth-Paul[37] has shown that it is more convenient to use the relation

$$\Delta\nu(PR) = 10\tilde{x}(\tilde{B}T/9)^{1/2} \text{ cm}^{-1} \qquad (30)$$

where $\tilde{x}$ is again either a number, a constant ratio or a function of molecular parameters given in Table 2[37], while $\tilde{B}$ = BC/(B + C) or AB/(A + B) depending upon whether the molecule is a prolate or an oblate asymmetric rotor respectively.

Thus equation (30) has been used in the present work to determine the PR separation of asymmetric rotors. The moments of inertia show all our molecules, except tristrifluoromethylphosphine to be prolate asymmetric rotors with κ and ρ^* lying between -0.52 - -0.84 and 0.97 - 1.55 respectively. Thus, from Table 2[36] $\tilde{x}$ values for A, B and C type bands are equal to $S(\tilde{\beta})$, 1 and $3S(\tilde{\beta})/2$ respectively, where $S(\tilde{\beta}) = 0.712/(\tilde{\beta} + 4)^{1.13}$ and $\tilde{\beta} + 1 = A/2\tilde{B}$.

Since the majority of molecules studied here have only a C_s symmetry, vibrational modes for which the dipole moment change occurs in the plane of symmetry will have a more or less hybrid structure and the PR separation given by formulae (30) will therefore not correspond to the experimental value. However Seth-Paul and De-Meyer[38] have given a formula for the calculation of PR separation of a hybrid band namely

$$\nu(\text{PR}) \text{ type } \alpha\beta = \left(\frac{\tilde{x}\tan\alpha + 1}{1 + \tan\alpha}\right) \cdot S_\alpha \text{ cm}^{-1} \qquad (31)$$

where S_α refers to the PR separation of a pure α type band and α to the angle between the direction of the oscillating dipole and minor α axis of inertia with respect to the other β axis. $\tilde{x}$ is either a number, a constant ratio or a function of several molecular parameters, depending on the value of κ and ρ^* and its values have been given in Table 2[38]. For our molecules since $-0.52 < \kappa < -0.84$ and $0.97 < \rho^* < 1.55$, x values from Table 2[38] for AB, AC and BC type bands are $1/8(\tilde{\beta})$, 3/2 and $3/2S(\tilde{\beta})$ respectively. According to Seth-Paul et al.[38] if $\alpha < \pi/4$, the hybrid band is denoted by $\alpha\beta\parallel$, while for $\pi/4 < \alpha < \pi/2$ the hybrid band is denoted by $\alpha\beta\perp$. It is this notation which has been used to describe the expected band types in Tables 2, 4, 6, 10, 12, 14 and 16.

Chapter 3

EXPERIMENTAL

This chapter gives details of the methods employed in the preparation and recording of the spectra of various compounds. The preparation of the compounds has been divided into two sections. Section 3.1 deals with the preparation of selenium compounds, while Section 3.2 deals with the preparation of phosphorus compounds. For each of these sections, a general review is given first, followed by the actual details.

3.1 The Selenium Compounds

All selenium compounds reported in this work have been prepared by the original methods[2,3,39] and the details described by Clase[8] and Bomford[9], which sometimes had to be modified. For most of the compounds the reactions employed are simple and unidirectional as evidenced by their high yields. Where any by-products were expected steps were taken to either ensure their absence or to purify the compound till its spectrum revealed it free of the intense bands of the by-products.

3.1.1 General

A homogeneous mixture of selenium and silver trifluoroacetate (molar ratio 1:5) is heated at 280° for two

hours in a pyrex tube, when the following reaction takes place[3]:

$$Se + CF_3COOAg \xrightarrow[2\ hrs.]{280^\circ} (CF_3)_2Se + (CF_3Se)_2 + COF_2 + SiF_4 + CO_2 + - - -$$

Bistrifluoromethyl selenide (b.p. = -2°) and diselenide (b.p. = 73°) are easily separated from other highly volatile components, silicon tetrafluoride and carbon dioxide etc. by vacuum fractionation. Bistrifluoromethyl selenide and diselenide are separated from each other by shaking the mixture with mercury in daylight for 24 hours[8], when bistrifluoromethyl diselenide reacts to form a yellow crystalline compound, bis(trifluoromethylseleno)mercury,

$$(CF_3Se)_2 + Hg \longrightarrow (CF_3Se)_2Hg$$

which serves as a useful intermediate in the synthesis of almost all other compounds whose spectra are being reported here. Bis(trifluoromethylseleno)mercury reacts at room temperature with chlorine[9], bromine[9], iodine[9] and methyl iodide[39] to form trifluoromethylselenenyl chloride, trifluoromethylselenenyl bromide, bistrifluoromethyl diselenide and methyl trifluoromethyl selenide respectively. The reactions can be summarised in terms of the following equations.

$$(CF_3Se)_2Hg + 2Cl_2 \rightarrow 2CF_3SeCl + HgCl_2$$

$$(CF_3Se)_2Hg + 2Br_2 \rightarrow 2CF_3SeBr + HgBr_2$$

$$(CF_3Se)_2Hg + I_2 \text{ (excess)} \rightarrow (CF_3Se)_2 + HgI_2$$

and $$(CF_3Se)_2Hg + 2CH_3I \rightarrow 2CF_3SeCH_3 + HgI_2$$

Finally, trifluoromethyl selenocyanate is prepared by the reaction between trifluoromethylselenenyl chloride and silver cyanide (9)

$$CF_3SeCl + AgCN \rightarrow CF_3SeCN + AgCl$$

The following cold baths have been used for performing vacuum fractionation.

Bath	Temperature °C
Liquid nitrogen	-196
75 per cent isopentane + 25 per cent n-pentane	-140
75 per cent n-pentane + 25 per cent isopentane	-150
Diethyl ether	-116
Acetone	- 95
Ethyl acetate	- 83
Dry ice + acetone	- 78
Chloroform	- 63
Ice + common salt	- 21

3.1.2 Preparation of Bis(trifluoromethylseleno)mercury

Trifluoromethyl silver acetate (14 g.) and selenium powder (18 g.) in the molar ratio 1:5 were thoroughly mixed in a mortar and the mixture dried in a vacuum over phosphorus pentoxide for three days.

In a typical experiment, 10 g. of this mixture were placed in a Carius tube (25 cm x 30 cm), which had been earlier flamed out under vacuum to remove traces of moisture. The tube was evacuated, sealed and heated in an oven at 280° for 120 minutes, after which time the tube was broken open in a vacuum line and the fraction volatile at -78° was pumped off and discarded. The fraction involatile at -78° was retained and condensed onto an excess of triply distilled mercury contained in a Carius tube. The tube was sealed and kept shaking in daylight for 24 hours. At the end of this time a black solid with a few yellow specks had formed in the tube. The tube was broken open on the vacuum line and the volatile products (mainly bistrifluoromethyl selenide) were sealed into another thick-walled tube. The black residue with a few yellow specks was extracted with anhydrous ether and the ether was later evaporated off giving a dirty yellow substance. This was sublimed at 50°, in the dark, to give a yellow crystalline substance having the melting point 50 - 51°. The yield of the final product in a typical experi-

ment was 1.73 g., a yield of 35 per cent based on CF_3 group. Since the amount of bis(trifluoromethylseleno)mercury obtained from one tube was quite small, the reaction was performed simultaneously in four tubes and the combined product treated as above. Since the compound undergoes slow decomposition in light, it was stored in the dark and always either prepared fresh or sublimed before use.

3.1.3 Preparation of Bistrifluoromethyl Selenide

The impure bistrifluoromethyl selenide collected in sub-section 3.1.2 was subjected to high vacuum fractional distillation in a vacuum line of conventional design having four traps. Three consecutive traps were maintained at -196, -116 and -95° respectively and the impure fraction was allowed to evaporate slowly from the trap at -95°. After sometime, nothing was left in the trap at -95°, while the major fraction collected in the trap at -116° and a very small amount collected in the trap at -196°. The above process was repeated several times till nothing collected in the trap at -196°. The contents of the trap at -116° were further purified by several trap-to-trap distillations rejecting the end 5 per cent fraction every time to ensure the complete removal of high boiling impurities, if present. Finally the pure bistrifluoromethyl selenide was sealed in a thick-walled glass ampoule under vacuum. The infrared

spectrum did not reveal any bands due to CO_2 and SiF_4.

3.1.4 Preparation of Trifluoromethyl Methyl Selenide

$$(CF_3Se)_2Hg + 2CH_3I \longrightarrow 2CF_3SeCH_3 + HgI_2$$

Methyl iodide was condensed into a weighed thick-walled pyrex glass tube, the tube sealed and reweighed. In this manner freshly distilled methyl iodide (2.96 g.) was condensed onto bis(trifluoromethylseleno)mercury (5.3 g., slight excess), contained in a thick-walled Carius tube. The tube was sealed and shaken for four days at room temperature. Crystals of red mercuric iodide appeared and a clear liquid separated. The product, volatile at room temperature, was transferred under vacuum to a weighed thick-walled tube. The product was found to weigh 3.2719 g., a 96.2 per cent yield. It did not reveal any bands due to CH_3I in the infrared.

3.1.5 Preparation of Bistrifluoromethyl Diselenide

$$(CF_3Se)_2Hg + I_2 \longrightarrow (CF_3Se)_2 + HgI_2$$

Bis(trifluoromethylseleno)mercury (3.0 g.) and iodine (1.7 g., excess), previously dried over phosphorus pentoxide, were sealed together in a Carius tube and the tube heated at 100°. After ten minutes of heating a yellow liquid and a red solid started to appear. The tube was heated for three hours to allow the completion of reaction.

The product volatile at room temperature was transferred under vacuum and sealed into a weighed thick-walled tube. The product was found to weigh 1.7223 g., a 96.3 per cent yield.

3.1.6 Preparation of Trifluoromethylselenenyl Chloride

$$(CF_3Se)_2Hg + 2Cl_2 \longrightarrow 2CF_3SeCl + HgCl_2$$

Dry chlorine gas (1.6176 g.) was condensed onto bis(trifluoromethylseleno)mercury (5.695 g.), contained in a Carius tube (in exact stoichiometry of 1:2) and the tube sealed. Bomford[9] has used bis(trifluoromethylseleno)mercury in excess of stoichiometry, which may lead to the reaction:

$$(CF_3Se)_2Hg + Cl_2 \longrightarrow (CF_3Se)_2 + HgCl_2$$

and hence give bistrifluoromethyl diselenide as impurity. As soon as the tube came to room temperature, a cherry red liquid started separating. The tube was kept at room temperature for 24 hours to allow the reaction to go to completion. To prevent the transfer of any trichloride that might have formed, only the product volatile at -21° was transferred under vacuum to a weighed thick-walled tube. The product was found to weigh 4.1586 g., a yield of 98 per cent.

3.1.7 Preparation of Trifluoromethylselenenyl Bromide

$$(CF_3Se)_2Hg + 2Br_2 \longrightarrow 2CF_3SeBr + HgBr_2$$

Bromine gas (1.9119 g.) was condensed onto

bis(trifluoromethylseleno)mercury (2.637 g.), contained in a Carius tube (in exact stoichiometry of 1:2) and the tube sealed. The stoichiometry is important for the reasons explained in sub-section 3.1.6. As soon as the tube came to room temperature, a dark brown liquid started separating. The tube was kept at room temperature for 24 hours to allow completion of reaction. The tube was then broken open on the vacuum line and the product volatile at -21° was transferred to a weighed thick-walled tube leaving behind a white residue consisting of mercuric bromide and may be a small amount of selenium tetrabromide. The product was found to weigh 2.3784 g., a yield of 87.3 per cent.

3.1.8 Preparation of Trifluoromethyl Selenocyanate

$$CF_3SeCl + AgCN \longrightarrow CF_3SeCN + AgCl$$

Trifluoromethylselenenyl chloride (1.8476 g.) was condensed onto an excess of dry silver cyanide, contained in a Carius tube. The tube was sealed, wrapped in an aluminium foil (to prevent photodecomposition of AgCN) and kept shaking for 24 hours. By the end of this time, the red colour of trifluoromethylselenenyl chloride had disappeared and a colourless liquid appeared. The tube was broken open on the vacuum line and the product volatile at room temperature transferred to a weighed thick-walled tube. The product was found to weight 1.7294 g., a yield of 98.7 per cent.

3.2 The Phosphorus Compounds

The perfluoromethyl compounds of phosphorus studied here have been prepared using methods of Bennett et al.[1], Burg and Brendel[40,41] and modifying them when and where felt necessary. The purity of the compounds was determined by comparing their infrared spectra with the already known part of the spectra of the pure compounds[1,42]. Where any by-products were expected all steps were taken to purify the compound till its spectrum revealed it free of the intense bands of the by-products.

3.2.1 General

When red phosphorus and trifluoromethyl iodide are heated together at 195 - 200° for 48 hours, the following reaction takes place.

$$P(red) + CF_3I \xrightarrow[48\ hrs]{195\text{-}200^\circ} P(CF_3)_3 + (CF_3)_2PI + CF_3PI_2 + PI_3 + P_2I_4$$

The following equilibrium is set up in reaction vessel:

$$(CF_3)_2PI \rightleftharpoons P(CF_3)_3 + CF_3PI_2$$

$$2CF_3PI_2 \rightleftharpoons (CF_3)_2PI + PI_3$$

$$P(CF_3)_3 + I_2 \rightleftharpoons (CF_3)_2PI + CF_3I$$

The yield of trifluoromethyliodophosphines increases with the use of low temperature and phosphorus tri-iodide in the

reactants[1]. The products, i.e., unreacted trifluoromethyl-iodide (b.p. =-22°), tristrifluoromethylphosphine (b.p. = 17.3°), bistrifluoromethyliodophosphine (b.p. =73°), trifluoromethyldi-iodophosphine (b.p. - 140°) and phosphorus iodides (solid) can be easily separated from each other by high vacuum fractionation.

Trifluoromethyliodophosphines thus obtained are converted to corresponding trifluoromethylfluorophosphines using antimony trifluoride as fluorinating agent and the method of Burg and Brendel[40,41] (after slight modifications), when the following metathetical reaction takes place

$$3(CF_3)_2PI + SbF_3 \longrightarrow 3(CF_3)_2PF + SbCl_3$$

$$3CF_3PI_2 + 2SbF_3 \longrightarrow 3CF_3PF_2 + 2SbCl_3$$

The method of Kulakova et al.[43] was found to be complicated and hence not used.

3.2.2 Purification of Reagents

Water and low boiling impurities (C_2F_6, air etc.) were removed from trifluoromethyl iodide by passing the gas through a set of three traps maintained at -116, -150 and -196° respectively and using the fraction condensing in the trap at -150°. Red phosphorus used was of commercial grade and was purified by refluxing portions of 100 g. for 24 hours

with 250 ml of 7 per cent sodium hydroxide solution under an atmosphere of nitrogen. After removal of the hydroxide the phosphorus was boiled for 24 hours with distilled water under an atmosphere of nitrogen. Later phosphorus was washed with cold water until alkalinity disappeared. Phosphorus was now washed with absolute ethanol to remove water and dried in a vacuum dessicator.

3.2.3 Preparation of Crude Tristrifluoromethyl- and Trifluoromethyliodophosphines

Trifluoromethyl iodide was weighed by condensing it into weighed thick-walled tubes, which were sealed and re-weighed.

In a typical experiment, dry purified red phosphorus (7.9 g.) was packed in a Carius tube (30 cm x 2.5 cm), which was evacuated for about four hours, heating occasionally to approximately 100° with flame to remove traces of water. Purified trifluoromethyl iodide (10 g.) was now condensed onto red phosphorus (molar ratio 5:1). The tube was evacuated, sealed and heated at 195 - 200° in an oven for 48 hours. The volatile contents of the tube were transferred to a vacuum line of conventional design fitted with a diffusion pump and having four traps (say 1, 2, 3 and 4 in order). Vacuum distillation was carried out by maintaining traps 4, 3 and 2 at temperatures of -196, -116 and -95° respectively and allowing

the liquid in the trap 1 to evaporate at reasonably slow rate. After everything had evaporated from trap 1, the largest amount collected in trap 4 (-196°), which the infrared spectrum revealed to be mostly trifluoromethyl iodide with a very little of tristrifluoromethylphosphine. The contents of traps 3 and 2 were equal by volume. The contents of trap 3 (-116°) were colourless. The infrared spectrum showed them to be mostly tristrifluoromethylphosphine with a little trifluoromethyl iodide and possibly some bistrifluoromethyliodophosphine as impurities. The contents of trap 2 were brownish yellow in colour and should be a mixture of trifluoromethyliodophosphines with a trace of free iodine as impurity. The contents of traps 4 and 3 were separately sealed into thick-walled glass ampoules. The contents of trap 2 were further separated in two components by maintaining two consecutive traps at -63° and -95° respectively, when a light yellow liquid collected in the trap at -95°. The infrared spectrum revealed it to be mostly bistrifluoromethyliodophosphine (colourless) with a little of trifluoromethyldi-iodophosphine (yellow). The trap at -63° contained a dark yellowish-violet liquid, which should be mostly trifluoromethyldi-iodophosphine with a trace of free iodine as impurity. Both these fractions were sealed into separate glass tubes and stored in dark at low temperature, to avoid photo-decomposition. Thus these fractions could not be weighed. However, the amount of trifluoromethyliodophosphine

was greater than that of trifluoromethyldi-iodophosphine by volume. Since the compounds are reactive all stopcocks were greased with halocarbon grease, Kel-F. All fractionations were carried out with vacuum line wrapped in Aluminium foil to avoid decomposition of unstable products. Since the amounts of products obtained from one tube were too small, especially the trifluoromethyldi-iodophosphine, the same reaction was carried out in four more tubes and the combined products treated as above.

3.2.4 Preparation of Tristrifluoromethylphosphine

The fraction which condensed into the trap at -116° in sub-section 3.2.3 contained trifluoromethyl iodide (low boiling) and might also contain bistrifluoromethyliodophosphine as high boiling impurity. So this fraction was further purified by several high vacuum distillations, till the infrared spectrum was free of trifluoromethyl iodide. In a typical fractionation, three consecutive traps were maintained at -95, -116 and -196° respectively. The impure tristrifluoromethylphosphine was slowly evaporated from the -95° trap and the final 5 per cent of the fraction in this trap was rejected each time to ensure complete removal of the high boiling impurity (bistrifluoromethyliodophosphine). Finally, the fraction in the trap at -116° was sealed into a weighed thick-walled pyrex glass tube as pure tristrifluoromethyl-

phosphine. The infrared spectrum compared well with already reported spectrum of pure compound[1].

3.2.5 Preparation of Bistrifluoromethylfluorophosphine

The fraction which finally condensed into the -95° trap in sub-section 3.2.3 might contain tristrifluoromethylphosphine and trifluoromethyldi-iodophosphine as impurities. This was therefore purified by several high vacuum distillations as described in sub-section 3.2.4, but still it had a very light yellow colour although infrared spectrum compared well with the already reported spectrum of the pure compound[1]. The purified fraction was condensed on freshly sublimed antimony trifluoride (2.5 g., excess by visual approximation), contained in a Carius tube and the tube sealed. According to Burg and Brendel[40], the reaction went to completion at room temperature in three days, but we found that at room temperature the reaction went to only about 10 per cent. Perhaps the ruby red coating of antimony tri-iodide, stopped antimony fluoride from further reaction. Thus to remove this inert coating of antimony tri-iodide a magnetic follower was put inside the tube, but still even in three days the reaction went to only 25 per cent. Finally, the tube was heated to 60° for 24 hours and it was found that the reaction went to almost 100 per cent. The volatile contents of the tube were transferred to the vacuum line and subjected to several vacuum

distillations, using three traps at -196, -140 and -116° respectively and the method described in sub-section 3.2.4. The major fraction collected in the trap at -140° (where bistrifluoromethylfluorophosphine was supposed to collect). A small unreacted fraction remained in the trap at -116° (which might be $P_2(CF_3)_4$)[40] and almost nothing collected in the trap at -180°. Finally, the fraction in the trap at -140° was sealed in a clean thick-walled tube as pure bistrifluoromethylfluorophosphine. The infrared spectrum did not reveal any intense bands due to $P_2(CF_3)_4$. Only one intense band was observed in the P-F stretching region at 852 cm^{-1}.[42]

3.2.6 Preparation of Trifluoromethyldifluorophosphine

The fraction which condensed in the -63° trap in sub-section 3.2.3, could not be further purified and perhaps contained in addition to trifluoromethyldi-iodophosphine iodine as impurity. Therefore, it was condensed as such on freshly sublimed antimony trifluoride (2 g., excess by visual approximation), contained in a Carius tube containing a magnetic follower. The tube was sealed and kept stirred for 36 hours at 60°, after which time colourless antimony trifluoride had changed to ruby-red antimony tri-iodide and no yellowish trifluoromethyldi-iodophosphine could be seen. Similar conditions have been reported in reference[41], but this was received late and hence could not be referred to when the compound was being prepared. The volatile contents of the

tube were now transferred to the vacuum line and subjected to several vacuum distillations, using three traps at -196, -150 and -140° respectively and the method described in sub-section 3.2.4. The major fraction collected in the trap at -150°, where trifluoromethyldifluorophosphine was supposed to collect. A very small amount collected in the trap at -196° (which may be PF_3) while nothing was left in the trap at -140°. Finally, the fraction condensing in the trap at -150° was sealed in a clean thick-walled glass tube as pure trifluoromethyl-difluorophosphine. The infrared spectrum did not reveal any intense bands due to PF_3. Only one intense band was observed in the P-F stretching region at 865 cm^{-1}.[42] Four typical reaction tubes gave about 0.5 g. of the final product.

3.3 Instrumentation

Gas phase infrared spectra between 4000 - 250 cm^{-1} were recorded on Perkin-Elmer model 457 grating infrared spectrophotometer, using 10 cm gas cells, fitted with CsI and NaCl windows respectively. If some bands were expected in the region 250 - 200 cm^{-1}, the region was scanned on Perkin-Elmer model 225 prism and grating spectrophotometer.

All spectra between 4000 - 600 cm^{-1} were recorded using normal slits (resolution of 4 and 2 cm^{-1} at 3000 and 1000 cm^{-1} respectively) and slow scan speeds. To record the overtone and combination bands, the gas cell was filled with the vapor pressure of the substance at - 45° for high boiling compounds. For the low-boiling compounds the pressure was adjusted to get a reasonable intensity for the overtones and combination bands. In no case, the pressure was allowed to exceed 760 mm at ≈ 45° and no attempt was made to record the pressure in the cell, since the compounds are reactive and attack mercury. Later, the pressure was reduced to record other important bands. The instrument was calibrated in the region 4000 - 600 cm^{-1} using polystyrene film and internal calibration (carbon dioxide and water bands[44]), while the region from 600 - 250 cm^{-1} was calibrated using water bands[45] (internal calibration). Bands which seemed to show a structure were recorded on ten times expanded abscissa, to

determine accurately the PR separations. The spectra between 600 - 250 cm^{-1} were always recorded on ten times expanded abscissa to determine the position of bands with better precision. Thus, the wavenumbers of various bands are reliable to $\pm$ 5, $\pm$ 3 and $\pm$ 2 cm^{-1} in the regions 4000 - 2000, 2000 - 600 and 600 - 250 cm^{-1} respectively, while the PR separations are accurate to $\pm$ 0.2 cm^{-1}. The instrument was always flushed with carbon dioxide-free, dry air to avoid absorption by carbon dioxide and water bands, especially in the region 600 - 250 cm^{-1}. All selenium compounds were dried over phosphorus pentoxide before recording their infrared and Raman spectra. Trifluoromethylselenyl chloride and bromide were found to attack CsI windows, the latter compound attacking more readily than the former. So, their spectra were recorded between 4000 - 700 cm^{-1} using NaCl cell, and between 600 - 250 cm^{-1} the CsI cell was used. The compounds attacked CsI windows and turned them yellow possibly through the following reaction

$$2CsI + 2CF_3SeX \longrightarrow (CF_3Se)_2 + 2CsX + I_2$$

(where X = Cl,Br)

The thin coating of the compound CsX was formed on the windows which prevented any further attack and consequent decomposition of CF_3SeX. The windows remained fairly transparent after the attack and did not show any absorption. Among the phosphorus compounds CF_3PF_2 and $(CF_3)_2PF$ were

found to attack CsI windows slowly, therefore the spectra of these were recorded between 4000 - 700 cm^{-1} using NaCl cell and between 600 - 250 cm^{-1} CsI cell was used. After attack CsI cell showed many absorptions in the region 1300 - 250 cm^{-1}, but no sign of attack appeared in the small time taken to record the spectra between 600 - 250 cm^{-1}.

The Raman spectra were recorded using a Coderg PH0 instrument equipped with Coherent Radiation Laboratories model 52 argon-krypton ion laser as the Raman source. The Raman spectra of all reported compounds were recorded as liquids in sealed thick-walled capillary tubes (4 mm o.d.), placed vertically in the appropriate laser beam depending on the colour of the compound. All compounds were colourless except $(CF_3Se)_2$, CF_3SeCl and CF_3SeBr, which had light-yellow, red and dark-brown colour respectively. The spectrum of CF_3SeCl was recorded using red laser line (154449.56 cm^{-1}). It was not possible to record the Raman spectrum of CF_3SeBr, However, some bands have earlier been recorded by using reflection from glass-liquid interface by Bomford[9]. So, the values reported by him have been used and these values agree well with the infrared values found in this study (Table 5). The Raman spectra of all other compounds, including $(CF_3Se)_2$ were recorded using blue line (20486.53 cm^{-1}) and slit setting of 2 cm^{-1}. However, the slits had to be

opened to 6 cm^{-1} to record the C-F stretchings, CF_3 asymmetric deformations and other weak and broad bands.

The instrument was calibrated using the plasma lines from the laser, whose wavelengths are reported up to two to four decimal places in the MIT tables[46]. Using Wang 720B advanced programmable calculator, a chart was prepared (Table 1) which serves the dual purpose of calibration as well as elimination of spurious lines appearing in the spectrum of an unknown compound. From Table 1, the Raman instrument was found to have an almost uniform deviation of -2 cm^{-1}. The wavenumbers of the Raman bands reported in Tables 2 - 19 are reliable to $\pm$ 2 cm^{-1}, unless the band is quite broad.

Table 1. Possible spurious lines emitted by the laser plasma of Model 52 argon-krypton ion laser, used as Raman source

Element	Discharge tube intensities	Observed path height	Wavelength in Angstroms in Standard Air	Frequency in Wavenumbers in Vacuum	Apparent Raman displacement of the emission lines in wavenumbers from the laser lines				
					Frequency of laser in wavenumbers in vacuum				
					20040.31	20134.91	19439.00	19196.27	17594.91	15449.34
Ar	300	20	4879.8600	20486.51	.00					
ArII	30	20	4806.7500	20182.71	193.79					
Ar	30	100	4933.2400	20265.02	221.50					
KrII	300	45	4965.5900	20218.42	272.11					
Ar	40	100	4965.1200	20134.91	351.62	.00				
Ar	20	55	4972.1400	20106.40	380.13	28.50				
Ar	200	100	5019.3100	19957.13	529.40	177.77				
KrII	100	30	5013.2900	19941.44	545.08	193.46				
ArI	50	100	5017.2300	19923.70	560.87	209.20				
KrII	100	45	5021.8800	19907.11	579.19	227.57				
KrII	200	100	5022.4000	19909.27	581.25	229.43				
Ar	200	100	5042.0700	19749.28	717.24	385.42				
KrII	250k1	25	5084.5200	19654.35	812.17	480.55				
KrII	400k1	93	5125.7300	19504.00	982.52	630.90				
ArI	20	90	5141.8100	19443.01	1043.51	691.84				
ArII	4	100	5145.2800	19429.90	1056.63	705.09	.00			
KrII	80	70	5144.8000	19368.97	1117.55	785.91	80.92			
XeI	4	10	5148.0400	19344.25	1142.27	790.65	85.64			
KrII	60kw	30	5186.9900	19273.66	1212.87	861.26	156.23			
"	"	40	5200.2200	19224.62	1261.90	910.28	205.27			
KrII	500	100	5208.3200	19194.72	1291.80	940.18	235.17	.00		
"	130	50	5217.4500	19161.14	1325.38	973.76	268.74	33.58		
"	12	10	5217.9300	19159.37	1327.15	975.53	270.52	35.35		
"	60	100	5229.5200	19116.91	1369.61	1017.99	312.98	77.81		
"	100h	40	5274.5000	18964.70	1519.82	1168.20	463.19	268.02		
Ar	20	100	5286.9200	18919.16	1577.16	1221.54	520.53	285.36		
ArII	10	10	5303.7700	18862.18	1644.34	1292.72	587.71	352.54		
KrII	200	100	5308.6400	18931.92	1634.60	1302.98	597.97	362.80		
"	60h1	50	5322.7700	18782.00	1704.52	1352.90	647.89	412.72		
"	500h	100	5333.4100	18744.53	1741.99	1390.37	685.36	450.18		
KrII	40h1	100	5346.7600	18697.73	1788.79	1437.17	732.16	496.99		
"	10h	25	5355.4500	18667.39	1819.13	1467.51	762.50	527.33		
Ar	10	10	5397.6000	18521.42	1964.90	1613.28	908.27	673.10		
KrII	300ahe	48	5418.4300	18450.42	2035.10	1684.48	979.47	744.30		
"	40	50	5438.6300	18381.89	2104.63	1753.01	1048.00	812.83		
KrII	80	100	5444.3400	18155.87	2130.65	1779.03	1074.02	838.85		
"	80ahe	80	5448.1700	18282.59	2203.93	1852.31	1147.30	912.13		
"	50	35	5499.5400	18178.30	2309.22	1956.60	1251.59	1016.41		
"	60	62	5522.9600	18101.20	2385.24	2033.61	1328.61	1093.43		
"	30	10	5525.4700	18099.55	2386.97	2035.35	1330.34	1095.17		
ArI	10	20	5552.7800	18004.08	2482.45	2130.82	1425.81	1190.64		
KrI	500	10	5562.2257	17973.44	2513.08	2161.46	1456.45	1221.28		
KrII	100	60	5568.6500	17952.70	2533.82	2182.20	1477.19	1242.02		
KrI	2,000	35	5570.2895	17947.42	2539.10	2187.48	1482.47	1247.30		
KrII	100h	60	5633.0200	17747.55	2738.97	2387.35	1682.34	1447.16		
Ar	2	10	5673.0100	17622.43	2864.07	2512.45	1807.44	1572.27		
KrII	400	100	5681.8000	17594.91	2891.61	2539.99	1834.98	1599.81	.00	
"	200ahe	90	5690.3500	17568.75	2917.77	2566.15	1861.14	1625.97	26.15	
"	60	25	5752.9800	17377.49	3109.03	2757.41	2052.40	1817.23	217.42	
"	100	64	5771.4100	17322.00	3164.51	2812.91	2107.89	1872.72	272.91	
KrII	2wh	10	5777.7200	17303.08	3183.44	2831.82	2126.81	1891.64	291.82	
"	100wh1	12	5860.7500	17057.95	3428.58	3076.95	2371.94	2136.77	536.96	
KrI	3,000	45	5870.9158	17024.41	3458.11	3106.49	2401.48	2166.31	566.49	
KrII	200	100	5992.2200	16683.70	3802.81	3451.21	2746.20	2511.02	911.21	
"	40	12	6022.2900	16600.12	3886.41	3534.78	2829.77	2594.60	994.79	
ArII	100	100	6114.9200	16348.43	4137.30	3785.97	3080.66	2845.79	1245.98	
KrII	50	17	6148.8000	16256.13	4230.30	3928.77	3223.74	2988.59	1388.77	
"	6he	12	6171.7700	16199.33	4288.18	3936.57	3231.54	2996.39	1396.57	
"	2	72	6172.0800	16197.52	4289.90	3937.38	3232.37	2997.20	1397.38	
ArII	15	22	6243.1300	16011.19	4473.16	4121.71	3416.71	3181.53	1581.72	
KrII	100	25	6303.6600	15859.42	4627.10	4275.48	3570.47	3335.30	1735.48	
ArI	100	15	6416.6100	15580.25	4906.27	4554.65	3849.64	3614.47	2014.65	
KrII	300	100	6420.1800	15571.59	4914.93	4563.31	3858.30	3623.13	2023.31	
"	90	35	6470.8900	15449.56	5036.96	4685.34	3980.33	3745.16	2145.34	.00
ArII	15	22	6483.1000	15420.47	5066.05	4714.43	4009.43	3774.25	2174.44	29.09
ArI	2	75	6510.9500	15354.51	5132.02	4780.39	4075.38	3840.21	2240.40	95.05
KrII	150	100	6570.0700	15216.16	5270.15	4918.52	4213.55	3978.34	2378.56	233.22
"	15	70	6605.0000	15135.87	5350.65	4999.03	4294.02	4058.85	2459.03	313.69
"	15h	17	6634.3600	15068.80	5417.63	5066.01	4361.00	4125.83	2526.01	380.67
ArII	30	100	6638.2400	15060.08	5426.44	5074.82	4369.81	4134.64	2534.82	389.48
ArII	20	100	6639.7200	15056.72	5429.80	5078.18	4373.17	4137.99	2538.18	392.83
"	100	100	6643.7900	15047.50	5439.02	5087.40	4382.39	4147.22	2547.40	402.06
"	10	50	6644.3600	15046.22	5440.31	5088.69	4383.68	4148.51	2548.35	403.00
"	30	100	6684.3600	14956.17	5530.35	5178.73	4473.72	4238.55	2638.73	493.39
ArI	100	100	6756.1000	14797.34	5689.18	5337.56	4632.53	4397.36	2797.54	652.20
ArII	10	100	6764.4100	14794.24	5692.28	5340.66	4635.63	4398.48	2798.64	655.31
KrII	100	100	6763.4100	14780.93	5705.59	5353.97	4648.94	4411.79	2811.97	668.63
"	80	100	6774.4100	14777.14	5707.38	5355.76	4650.75	4413.59	2813.77	670.42
"	50	70	6771.2700	14764.37	5722.20	5370.58	4665.57	4428.40	2828.59	685.24
ArII	8	75	6861.1000	14570.48	5916.04	5564.42	4859.41	4624.24	3024.42	879.08
ArII	15	100	6863.5200	14565.37	5920.75	5569.13	4864.12	4628.95	3029.13	883.79
ArI	150	100	6871.2900	14549.30	5937.29	5585.60	4880.59	4645.42	3045.61	900.26
ArII	15	100	6896.1700	14517.02	5969.51	5617.88	4912.87	4677.70	3077.89	932.54
KrII	10h1	20	6964.0600	14374.81	6091.69	5738.07	5033.06	4797.89	3198.07	1052.71
ArI	400	100	6965.4300	14357.88	6133.84	5780.24	5077.21	4842.04	3242.24	1096.90

Chapter 4

APPROXIMATIONS AND ERRORS

Before proceeding to the discussions of the results it is important to stress the approximations underlying the calculations of the PR separations and the amount of error expected. Calculations for moments of inertia and PR separations were carried out using formulae laid down in Chapter 2.

4.1 Approximations

(i) Among the molecules studied here only $(CF_3)_2Se$, $(CF_3Se)_2$, CF_3SeCN and $P(CF_3)_3$ have been studied by electron diffraction[47,48,49,50] and the following values reported for the molecular parameters: $(CF_3)_2Se$, C-F = 1.334 ± 0.004, C-Se = 1.975 ± 0.009Å, $\angle FCF$ = 108.6 ± 0.4, $\angle CSeC$ = 97.0 ± 2.0 and an angle of twist of CF_3 groups = 26.7 ± 1°, $(CF_3Se)_2$, C-F = 1.326 ± 0.005, C-Se = 2.018 ± 0.020, Se-Se = 2.292 ± 0.01Å, $\angle FCSe$ = 109.1 ± 0.8, $\angle CSeSe$ = 98.0 ± 5°, $\angle CSeSeC$ dihedral = 84.5 ± 3.0° and an angle of twist of 11.8 ± 1.0° for both CF_3 groups from the conformation in which they are staggered with respect to the Se-Se bond; CF_3SeCN, C-F = 1.332 ± 0.007, Se-C(F_3) = 1.984 ± 0.020, Se-C(N) = 1.854 ± 0.016, N-C = 1.152 ± 0.020Å and $\angle CSeC$ = 92.2 ± 2°; $P(CF_3)_3$,

C-F = 1.342 ± 0.013, C-P = 1.937 ± 0.017, P..F = 2.715 ± 0.020Å and /CPC = 99.6 ± 2.5°. For other molecules no structural determinations have been attempted earlier. Hence, for these molecules, the molecular parameters are borrowed from structurally related molecules either as such or after slight modifications. To simplify moments of inertia calculations a suitable orientation of the CF_3 groups was selected and Figures 1, 2, 3, 5, 9, 10, 11 and 12 depict these orientations of the CF_3 groups in appropriate molecules. This simplifying procedure should not affect the values of moments of inertia themselves.

For the molecules CF_3SeCl, CF_3SeBr and CF_3SeCH_3, parameters for the CF_3Se group are borrowed as such from CF_3SeCN[48]. The parameters for Se-CH_3 group in the molecule CF_3SeCH_3 are borrowed from $(CH_3)_2Se$, which has been subjected to microwave study[51]. A value of 97° is assumed for the CSeC angle. The CSeC angle in $(CH_3)_2Se$ has been found to be 96.2°. Molecules Se_2Cl_2 and Se_2Br_2 have been studied by electron diffraction[52] and Se-Cl and Se-Br bonds have been found to be 2.13 and 2.24Å respectively. Thus, these values are borrowed as such for the appropriate molecules. /CSeX (X = Cl, Br) is assumed to be 92.5°, same as in CF_3SeCN.

For the phosphorus compounds $(CF_3)_2PF$ and CF_3PF_2, the molecular parameters for the CF_3 groups are borrowed as such from $P(CF_3)_3$, while the P-F bond distances are borrowed from PF_3 [53]. Since the /FPF in PF_3 has been found to be of similar magnitude to the /CPC in $P(CF_3)_3$, a value of 99.6° has been assumed for the /CPC = /FPF = /FCP (which has also simplified moments of inertia calculations). (ii) The calculations for the PR separations do not take into consideration effects due to centrifugal stretching, coriolis coupling and the change in rotational constants on going from the ground to the excited state.

As seen from above, the bond lengths have an uncertainty of 0.3 - 1 per cent even for the molecules studied by electron diffraction. Thus a minimum of 0.3 - 1 per cent error is expected in the moments of inertia of these molecules, which will lead to an error of similar magnitude in the predicted PR separations, even when factors mentioned in (ii) are not taken into account. However, if factors mentioned in (i) and (ii) are taken into account, they could lead to as much as 10 per cent error in the predicted values of PR separations. Since it is not possible to measure PR separations with an accuracy better than $\pm$ 0.2 cm^{-1}, therefore the calculated PR separations are being reported after rounding them off to first decimal place.

Chapter 5

RESULTS AND DISCUSSIONS

This chapter has also been divided into three sections. Sections 5.1 and 5.2 deal with selenium and phosphorus compounds respectively. If some work has earlier been done on these compounds or some important traits reported in similar compounds, they are given under the heading "General". Also given under this heading is the procedure followed to report and discuss experimental and calculated data and other characteristics common to all compounds.

5.1 The Selenium Compounds

5.1.1 General

All selenium compounds, except CF_3SeCH_3, for which the infrared and Raman spectra are being reported and discussed in the following pages, have earlier been studied in some detail by Bomford[9]. His assignments are mainly based on analogy with the spectra of closely related molecules and on depolarisation ratios. The following assignments have been made by him.

	CF_3SeCl	CF_3SeBr	CF_3SeCN	$(CF_3)_2Se$	$(CF_3Se)_2$
C-F asym. str.	1177	1175	1195	1192	1178,1115
C-F sym. str.	1106	1105	1101	1168	1090
CF_3 sym. def.	745	744	749	747	745
CF_3 asym. def.	542	?	530	532	530
C-Se stretch	336	?	?	?	327
Se-Se stretch	-	-	-	-	295
C-Se-C bend	-	-	-	114	110

All his assignments appear to agree with the present work, although the wavenumbers of some bands are somewhat different from ours. He has not tried to observe the splitting for the otherwise degenerate modes, which might be detectable in some cases. Further, in the case of molecules having two CF_3 groups, he has not made any distinction between the in-phase and out-of-phase modes.

The present study is more detailed and was undertaken with a view to make as many more assignments as possible. As will be seen subsequently, all assignments except for the torsional modes, which are generally weaker in the Raman have been made, although a few of them are tentative. The gas-phase infrared spectra have been recorded down to 200 cm^{-1}, with a view to study in detail the band contours, particularly where they show some structure. The study of band contours

has helped both in strengthening earlier assignments and making new assignments. The expanded scale spectra of some important bands are shown in Figures 4(a), 4(b), 8(a) and 8(b).

The calculated moments of inertia show all molecules, except $P(CF_3)_3$, to be prolate asymmetric rotors. Thus A∥, B⊥, C⊥ and hybrid type infrared bands are expected. The asymmetry parameters κ, ρ^* and β lie between -0.52 to -0.84, 0.97 - 1.56 and 0.73 - 1.36 respectively. The A∥ bands in general should have prominent PQR structure and the intensity of the Q branch should decrease as κ deviates from -1 (the symmetric rotor case). The C⊥ bands for $\kappa = -1$ should show only a prominent Q branch with weaker P and R branches, for values of $\beta < 1$, while for $\beta > 1$ the band envelope should no longer present the appearance of three maxima. As κ deviates from -1, the C⊥ type band takes up the features of an A∥ type band. The B⊥ type bands in general show a central minimum, provided this feature is resolvable. The central minimum will disappear as κ approaches -1. For $\kappa = -1$, the band will take the shape of a C⊥ band.

Torsional modes have not been observed for any of the molecules studied here, for generally they are weak in the Raman. Thus, either they are too weak to appear or lie below the limit ($\simeq 50$ cm^{-1}), below which it is not possible

to go because of Rayleigh scattering. Since all fundamentals in the molecules about to be discussed, lie in the narrow region (50 - 1300 cm^{-1}), vibrations of the same symmetry, in close proximity will show considerable mixing of valence coordinates in some normal modes. Hence, the descriptions of vibrations in all subsequent tables are only approximate. The number of vibrational modes, their symmetry type, assumed or established geometry, the calculated rotational constants and the expected PR separations for each molecule, if not given in the text are shown on the page preceding the description of the appropriate infrared and Raman spectra (Tables, 3, 5, 7, 9, 11, 13, 15, 17 and 19). For each molecule, the projection in a particular plane and calculated directions of inertial axes relative to the molecule in this plane are shown (Figures 1, 2, 3, 5, 9, 10, 11 and 12). Typical infrared and Raman spectra are shown in Figures 6 and 7 respectively. Assignments in Tables 2, 4, 6, 8, 10, 12, 14, 16 and 18 are based where possible on gas-phase infrared wavenumbers. Also, the discussions in the text unless mentioned are based on infrared wavenumbers. Herzberg's convention has been followed in numbering the vibrations.

5.1.2 Trifluoromethylselenenyl- chloride, bromide and cyanide

It is advantageous to discuss all these molecules first together as they are the simplest and similar to each

other, in that a trifluoromethylseleno group is attached either to a halogen or pseudohalogen and indeed they have similar spectra. Bomford[9] has shown the molecules to be bent at selenium, and to have C_s symmetry (by counting the number of bands in the Raman). From Figures 1, 2 and 3 it

Molecular parameters: C-F = 1.332, Se-Cl = 2.13Å, $\angle FCF$ = 109.3 and $\angle CSeC$ = 92.2°.

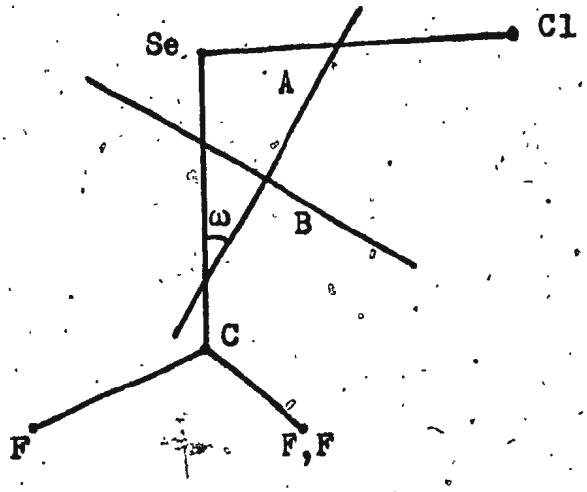

Figure 1. Projection of CF_3SeCl in the plane of symmetry along with the directions of inertial axes in this plane.

is obvious that all in-plane (a') and out-of-plane (a") normal modes of vibration should give AB hybrid and C⊥ type infrared band contours respectively.

In these molecules, the internal modes of the CF_3Se group can be easily assigned by comparing it to the CF_3Br

Molecular parameters: C-F = 1.332, Se-C = 1.984, Se-Br = 2.24Å, /FCF = 109.3 and /CSeC = 92.2°.

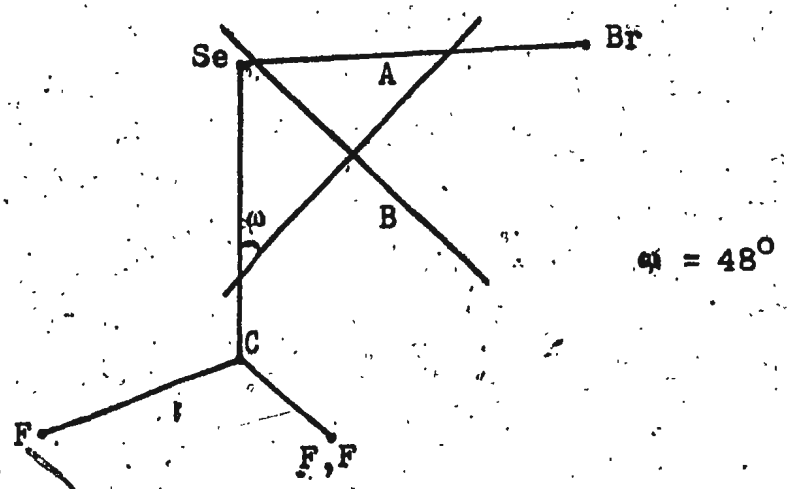

Figure 2. Projection of CF_3SeBr in the plane of symmetry along with directions of inertial axes in this plane.

Molecular parameters: C-F = 1.332, Se-C(F_3) = 1.984, Se-C(N) = 1.854, C≡N = 1.152Å, /FCF = 109.3 and /CSeC = 92.2°.

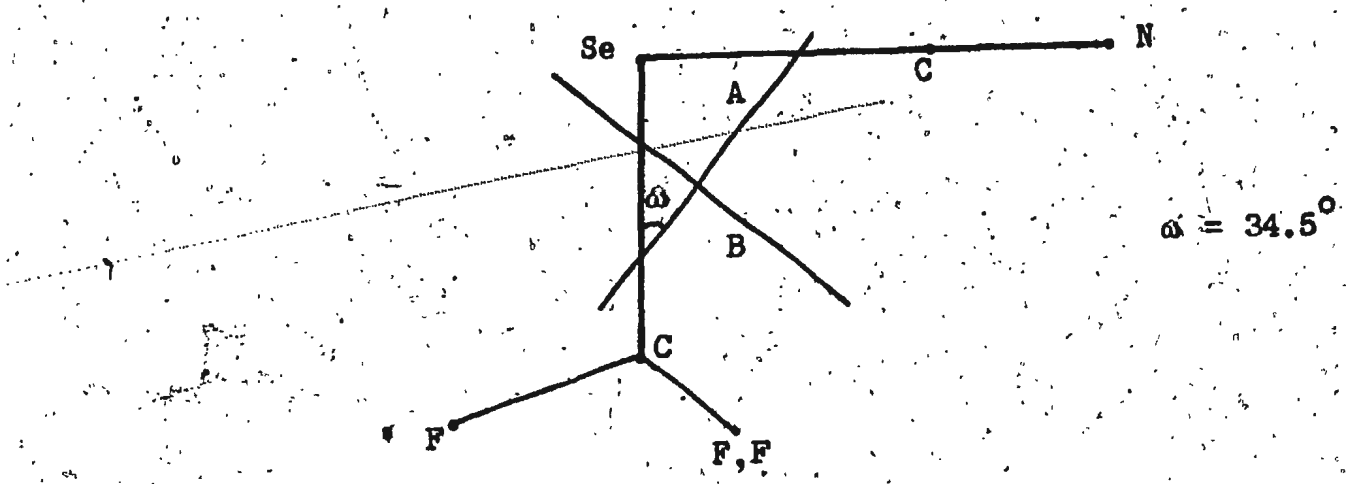

Figure 3. Projection of CF_3SeCN in the plane of symmetry along with the directions of inertial axes in this plane.

molecule, which has been thoroughly studied. The only difference being that each doubly degenerate (e) mode of CF_3Br should in principle split into a' and a" modes, due to lower C_s overall symmetry of the present molecules. In the C-F stretching region two intense absorptions are observed for each of these molecules. The lower wavenumber band is ascribed to $\nu_2(a')$, the symmetric C-F stretching mode. The band shows a slightly perturbed PQR structure {(Figure 4(a)} with PR separations of 10.5 (10.5), 8.5 (8.3) and 11.5 (10.5) cm^{-1} for the molecules CF_3SeCl, CF_3SeBr and CF_3SeCN respectively. For each molecule, the predicted value of PR separation is enclosed within brackets and shows good agreement with the experimental value. The corresponding Raman band in every case is weak and polarised. $\nu_1(a)$ in CF_3Br is found at 1085 cm^{-1}. The higher wavenumber band is assigned to asymmetric stretching mode, which is doubly degenerate and found at 1206 cm^{-1} in CF_3Br. The degeneracy for the C-F stretching mode seems to have slightly lifted in our molecules as the higher wavenumber band in all cases shows a sub-band structure {Figure 4(a)} with a' and a" modes strongly overlapped. For this band the first minimum on the higher wavenumber side is arbitrarily assigned to the origin of the AB⊥ type band contour expected out of the $\nu_1(a')$ mode. The maximum is then taken to be the Q branch of

the C⊥ type band, expected out of the a" component. This assignment is further confirmed by the Raman spectra, which shows a corresponding depolarised band.

The CF_3 asymmetric deformation mode is degenerate in CF_3Br and found at 550 cm^{-1}. Thus, the bands between 535 - 550 cm^{-1} in all these molecules are ascribed to CF_3 asymmetric deformation modes. For CF_3SeCl and CF_3SeBr, the band shows a sub-band structure with a' and a" modes overlapping each other. The asymmetric deformation modes seem to show more splitting compared to the asymmetric stretching modes. Again as before the first minimum on the higher wavenumber side is arbitrarily assigned to $\nu_4(a')$ mode, while the maximum at lower wavenumber end is assigned to the Q branch of the a" component. In the case of CF_3SeCl, the Raman spectrum in this region just shows one depolarised band. Thus the a' mode is either hidden under (the Raman bands in this region are weak and broad) or too weak to appear. Aynsley et al.[54] have studied the vibrational spectra of CH_3SeCN and assigned the strong intensity band in the infrared at 519 cm^{-1} to Se-C(N) stretching mode. We have observed for CF_3SeCN a strong intensity flat bottomed band with band centre at 538 cm^{-1}. The band is perhaps made up of two or three closely spaced bands. For all other molecules only weak intensity bands are observed in this region. Thus

the band at 538 cm^{-1} is perhaps made up of two or three closely spaced bands and therefore assigned to a composite of strongly overlapping (a' + a") CF_3 asymmetric deformations and Se-C(N) stretching modes. The Raman spectrum shows two weak but polarised bands in this region. By comparison with other single CF_3 group containing molecules whose spectra is being discussed here, the lower wavenumber band at 532 cm^{-1} is assigned to $\nu_4(a')$, the asymmetric deformation mode. The other $\nu_{12}(a")$ is possibly too weak to appear in the Raman. The higher wavenumber band is assigned to $\nu_5(a')$, the (N)C-Se stretching mode.

The band between 740 - 750 cm^{-1} in each of them is assigned to $\nu_3(a')$, the CF_3 symmetric deformation mode. It shows a good PQR structure {Figure 4(a)} expected of an AB|| type band contour, with a PR separation of 10.4 (10.5), 8.1 (8.3) and 11.0 (10.5) cm^{-1} for CF_3SeCl, CF_3SeBr and CF_3SeCN respectively. The predicted values of PR separation are enclosed within brackets and show a very good agreement with the experimental value in each case. The corresponding Raman band is always strong confirming the assignment. $\nu_2(a)$ for CF_3Br is found at 760 cm^{-1}.

By comparison among themselves and other selenium compounds studied here, the rocking modes are assigned to the bands appearing between 250 to 300 cm^{-1} (cf. 300 cm^{-1} for

Molecule = CF_3SeCl Symmetry type = C_s

Number of normal modes of vibration = 12

Symmetry species of the modes = 8a' + 4a"

Selection rules (for forbidden vibrations)

Infrared = none; Raman = none

Calculated principal moments of inertia (cm^{-1})

A = 0.0962, B = 0.0505, C = 0.0402

Calculated PR separations (cm^{-1}) and asymmetry parameters

A∥ = 11.4, B⊥ = 8.8, C⊥ = 17.2; κ = -0.63, $\rho^{\#}$ = 1.11

Table 2. Fundamental modes of CF_3SeCl, their assignments and expected band contour types.

Species	a'			a"		
Approximate description	Vib.	cm^{-1}	Band type	Vib.	cm^{-1}	Band type
C-F asym. stretch	ν_1	1180	AB⊥	ν_9	1185	C⊥
C-F sym. stretch	ν_2	1111	AB∥			
CF_3 sym. deformation	ν_3	744	AB∥			
CF_3 asym. deformation	ν_4	543	AB⊥	ν_{10}	539	C⊥
Se-Cl stretch	ν_5	429	AB⊥			
C-Se stretch	ν_6	336	AB∥			
CF_3 rock	ν_7	280	AB⊥	ν_{11}	250	C⊥
C-Se-Cl bend	ν_8	129	AB⊥			
CF_3 torsion				ν_{12}	?	C⊥

Table 3. Infrared and Raman spectra of CF_3SeCl

IR(gas)			Raman (liquid)			
I	cm^{-1}		cm^{-1}	pol.	I	Assignment
			129	dp	m	ν_8
			250	p	vw	ν_{11}
vw	280		278	p	vs	ν_7
m	336		335	p	s	ν_6
s	429		421	p	vs	ν_5
s	434		427	p	vs	
w	539	Q	539	dp	vw	ν_{10}
						ν_4
vw	547					
vvw	556					$2\nu_7 = 560$
vvw	566					?
vvw	585					$\nu_6 + \nu_{11} = 586$
vs	738	P				
vs	744	Q	744	p	s	ν_3
vs	749.2	R				
w	1025					$\nu_3 + \nu_7 = 1024$
s	1081		1074	p	vvw	$\nu_3 + \nu_6 = 1080$
vs	1106	P				
vs	1111	Q	1095	p	vw	ν_2
vs	1116.5	R				

Table 3. (Continued)

IR(gas)		Raman (liquid)				
I	cm^{-1}		cm^{-1}	pol.	I	Assignment
vw	1146					?
vs	1180	Q	1167	dp	vvw	ν_1
vs	1185					ν_9
vs	1187					
s	1228					$\nu_2 + \nu_8 = 1240$
m	1276					$\nu_3 + \nu_{10} = 1283$
m	1294					$\nu_3 + \nu_4 = 1287$
w	1390					$\nu_2 + \nu_7 = 1391$
w	1454					$\nu_1 + \nu_7 = 1460$
vw	1520					$\nu_6 + \nu_9 = 1521$
vw	1718					$\nu_1 + \nu_{10} = 1719$
w	1861					$\nu_1 + \nu_3 = 1855$
w	1924					$\nu_1 + \nu_3 = 1924$
w	2220					$2\nu_2 = 2222$
m	2285					$\nu_1 + \nu_2 = 2291$
w	2360					$2\nu_1 = 2360$

w = weak, m = medium, s = strong,
vs = very strong, mw = medium weak, ms = medium strong,
vw = very weak, vvw = very very weak, p = polarised,
dp = depolarised, I = intensity.

Molecule = CF_3SeBr Symmetry type = C_s

Number of normal modes of vibration = 12

Symmetry species of the modes = 8a' + 4a"

Selection rules (for forbidden modes)

Infrared = none; Raman = none

Calculated principal moments of inertia (cm^{-1})

A = 0.0845, B = 0.0357, C = 0.0289

Calculated PR separations (cm^{-1}) and asymmetry parameters

$A_{\parallel}$ = 9.4, $B_{\perp}$ = 7.5, $C_{\perp}$ = 14.2; κ = -0.75, $\rho^{\#}$ = 1.55

Table 4. Fundamental modes of CF_3SeBr, their assignment and expected band contour types.

Species	a'			a"		
Approximate description	Vib.	cm^{-1}	Band type	Vib.	cm^{-1}	Band type
C-F asym. stretch	ν_1	1177	AB$_{\perp}$	ν_9	1173	C$_{\perp}$
C-F sym. stretch	ν_2	1106	AB$_{\perp}$			
CF_3 sym. deformation	ν_3	745	AB$_{\parallel}$			
CF_3 asym. deformation	ν_4	534	AB$_{\perp}$	ν_{10}	530	C$_{\perp}$
Se-Br stretch	ν_5	332	AB$_{\parallel}$			
C-Se stretch	ν_6	324	AB$_{\parallel}$			
CF_3 rock	ν_7	285	AB$_{\perp}$	ν_{11}	264	C$_{\perp}$
CSeBr bend	ν_8	?	AB$_{\perp}$			
CF_3 torsion				ν_{12}	?	C$_{\perp}$

Table 5. Infrared and Raman spectra of CF_3SeBr

IR(gas)			Raman (liquid)			
I	cm^{-1}		cm^{-1}	pol.	I	Assignment
vw	264		254	p	w	ν_{11}
vw	285		266	p	vs	ν_7
s	324		324	p	s	ν_6
m	332		338	p	s	ν_5
vvw	360					$\nu_2 - \nu_3 = 361$
vvw	423					$\nu_9 - \nu_3 = 428$
w	530	Q				ν_{10}
						ν_4
vw	538					
vw	548					$\nu_7 + \nu_{11} = 549$
vw	585					$\nu_6 + \nu_{11} = 588$
vs	741	P				
vs	745	Q				ν_3
vs	749	R				
s	774					$\nu_1 - \nu_5 = 774$
w	1014					$\nu_3 + \nu_{11} = 1009$
m	1072					$\nu_3 + \nu_6 = 1077$
vs	1102.5	P				
vs	1106	Q				ν_2
vs	1111	R				
vw	1146					?

Table 5. (Continued)

IR(gas)		Raman (liquid)			
I	cm^{-1}	cm^{-1}	pol.	I	Assignment
vs	1173	Q			ν_9
vs	1177.5				ν_1
s	1274				$\nu_3 + \nu_4 = 1279$
vw	1367				$\nu_2 + \nu_{11} = 1370$
vw	1375				?
vw	1389				$\nu_2 + \nu_7 = 1391$
w	1445				$\nu_1 + \nu_{11} = 1441$
vw	1496				$\nu_1 + \nu_6 = 1501$
w	1713				$\nu_1 + \nu_4 = 1715$
w	1853				$\nu_2 + \nu_3 = 1851$
w	1920				$\nu_1 + \nu_3 = 1922$
w	2215				$2\nu_2 = 2212$
m	2280				$\nu_1 + \nu_2 = 2283$
w	2345				$2\nu_1 = 2354$

Molecule = CF_3SeCN Symmetry type = C_s

Number of normal modes of vibration = 15

Symmetry species of the modes = 10a' + 5a"

Selection rules (for forbidden vibrations)

Infrared = none; Raman = none

Calculated principal moments of inertia (cm^{-1})

A = 0.0893, B = 0.0515, C = 0.0394

Calculated PR separations (cm^{-1}) and asymmetry parameters

$A_{\parallel}$ = 11.5, $B_{\perp}$ = 8.8, $C_{\perp}$ = 17.3; κ = -0.52, $\rho^{\#}$ = 0.97

Table 6. Fundamental modes of CF_3SeCN, their assignments and expected band contour types.

Species	a'			a"		
Approximate description	Vib.	cm^{-1}	Band type	Vib.	cm^{-1}	Band type
C≡N stretch	ν_1	2178	AB⊥			C⊥
C-F asym. stretch	ν_2	1201	AB⊥	ν_{11}	1197	C⊥
C-F sym. stretch	ν_3	1103	AB∥			
CF_3 sym. deformation	ν_4	747	AB∥			
(N)C-Se stretch	ν_5	543	AB⊥			
CF_3 asym. stretch	ν_6	532	AB⊥	ν_{12}		C⊥
Se-C N bend	ν_7	390	AB∥	ν_{13}	354	C⊥
(F_3)C-Se stretch	ν_8	315	AB∥			
CF_3 rock	ν_9	273	AB⊥	ν_{14}	248	C⊥
C-Se-C bend	ν_{10}	118	AB⊥			
CF_3 torsion				ν_{15}	?	C⊥

Table 7. Infrared and Raman spectra of CF_3SeCN

IR(gas)			Raman (liquid)			
I	cm^{-1}		cm^{-1}	pol.	I	Assignment
			118	dp	m	ν_{10}
			248	p	vw	ν_{14}
vw	268		273	p	w	ν_9
			281	dp	vw	$\nu_7 - \nu_{10} = 278$
m	309	P				
m	315	Q	314	p	vs	ν_8
m	319	R				
w	337					
			354	dp	vw	ν_{13}
m	386					ν_7
m	393.5		396	p	vw	
w	486					$2\nu_{14} = 496$
w	497					$\nu_4 - \nu_{14} = 499$
s	538		532	p	m	ν_6
			543	p	w	ν_5
vw	589					$\nu_8 + \nu_9 = 588$
w	628					$2\nu_8 = 630$
vs	741	P				
vs	747	Q	749	p	vs	ν_4

Table 7. (Continued)

IR(gas)			Raman (liquid)			
I	cm^{-1}		cm^{-1}	pol.	I	Assignment
vs	752	R				
w	772					$\nu_6 + \nu_{14} = 780$
w	1064		1060	p	vvw	$\nu_4 + \nu_8 = 1062$
vs	1098.5	P	1094	p	vw	
vs	1103	Q	1102	p	vw	ν_3
vs	1110	R				
vs	1197	Q	1186	dp	vvw	ν_{11}
vs	1203					ν_2
s	1282					$\nu_4 + \nu_6 = 1279$
s	1290					$\nu_4 + \nu_5 = 1290$
w	1372					$\nu_3 + \nu_9 = 1375$
vw	1418					$\nu_3 + \nu_8 = 1418$
vw	1470					$\nu_2 + \nu_9 = 1474$
vw	1737					$\nu_5 + \nu_{11} = 1740$
w	1853					$\nu_3 + \nu_4 = 1850$
w	1943					$\nu_2 + \nu_4 = 1948$
			2176	p	s	ν_1
w	2200					$2\nu_3 = 2206$
m	2300					$\nu_2 + \nu_3 = 2304$
w	2386					$2\nu_2 = 2402$

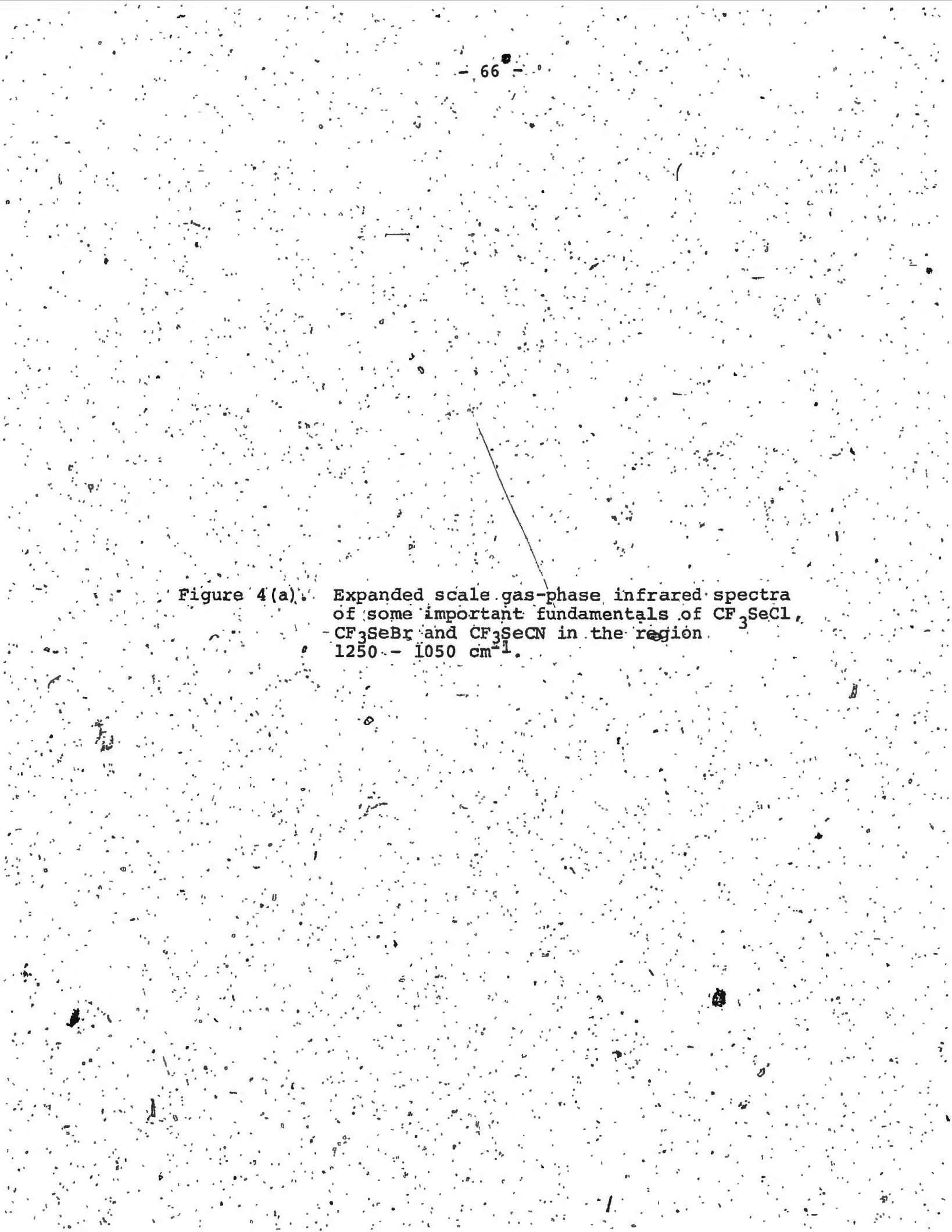

Figure 4(a). Expanded scale gas-phase infrared spectra of some important fundamentals of CF_3SeCl, CF_3SeBr and CF_3SeCN in the region 1250 - 1050 cm^{-1}.

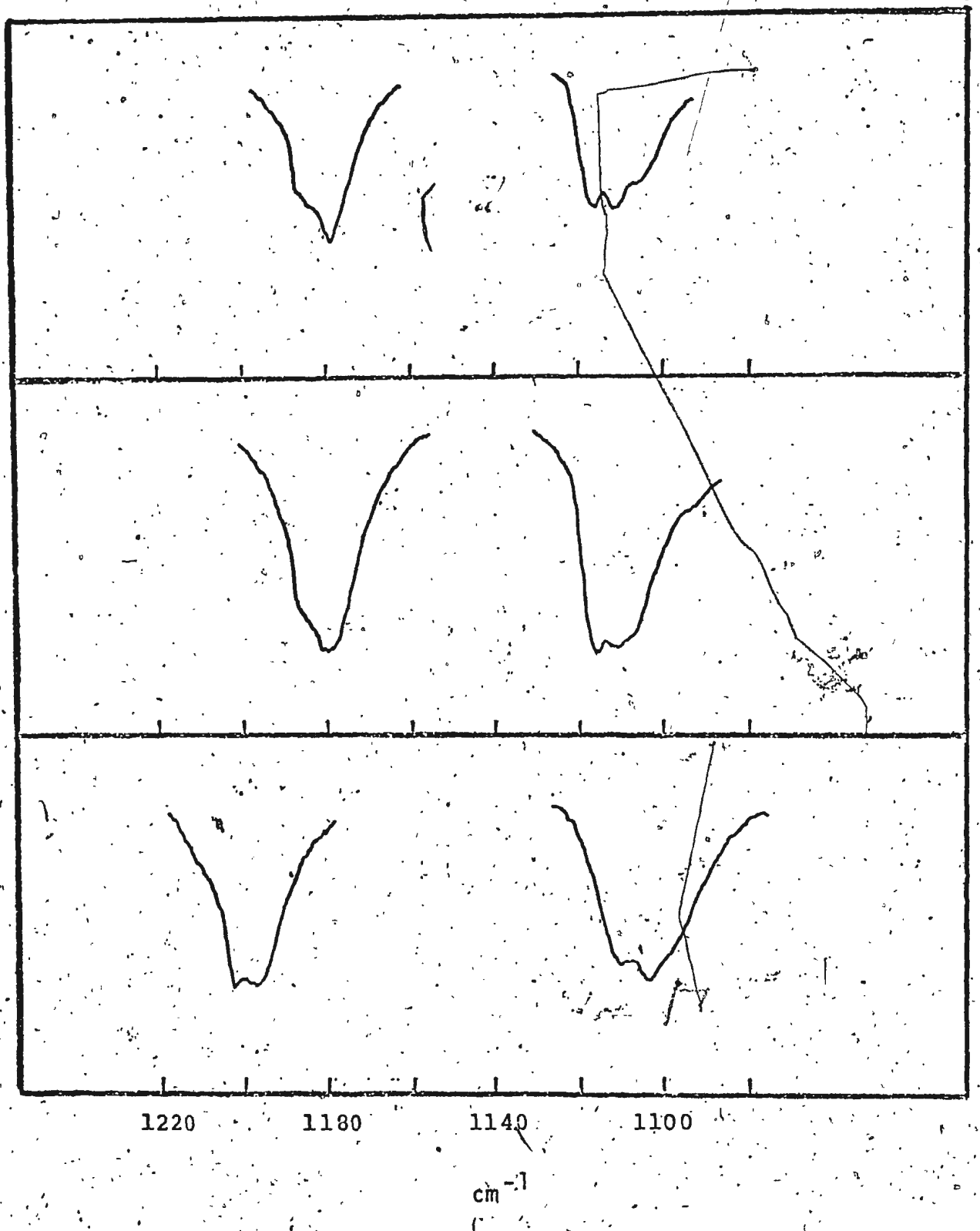

Figure 4 (a)

Figure 4(b). Expanded scale gas-phase infrared spectra of some important fundamentals of CF_3SeCl, CF_3SeBr and CF_3SeCN in the region 800 - 250 cm^{-1}.

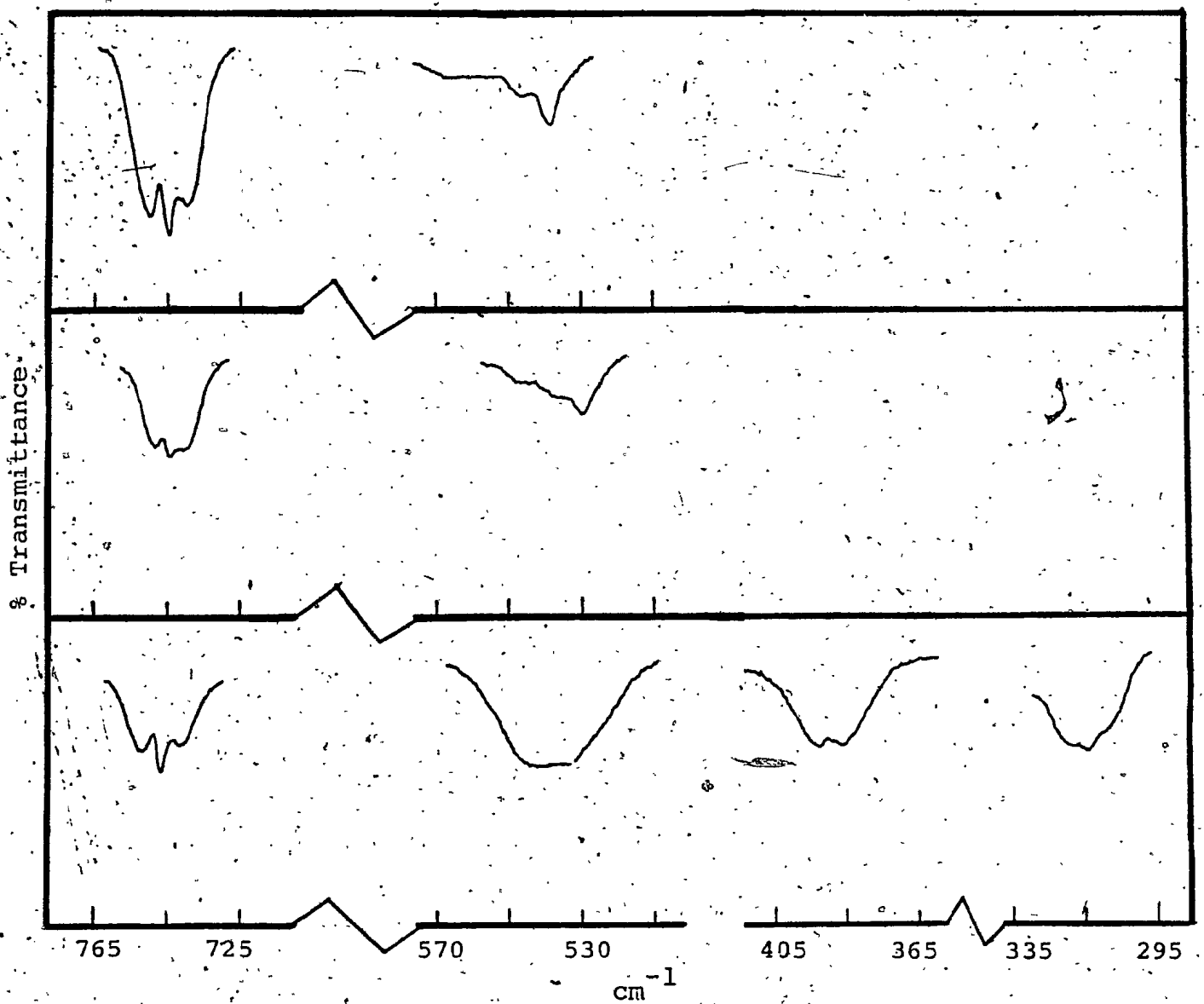

Figure 4 (b)

CF_3Br). The largest amount of splitting occurs for these rocking modes. In each case two bands appear in the Raman spectra in this region. The higher wavenumber band is always definitely polarised and much stronger than the lower wavenumber band. Thus the higher and lower wavenumber bands are ascribed to the in- and out-of-plane rocking modes respectively. The lower wavenumber band for both CF_3SeCl and CF_3SeCN seems to be polarised, although theoretically it should be depolarised. Since it is weak the depolarisation ratio cannot be determined accurately.

Coming to the skeleton vibrations, the medium intensity band appearing between 300 - 350 cm^{-1} is assigned in each case to the $(F_3)C$-Se stretching mode. It shows a PQR structure {Figure 4(b)} only in the case of CF_3SeCN with a PR separation of 10 cm^{-1}. The predicted PR separation of an AB|| type band is 10.5 cm^{-1}. The corresponding Raman band is always strong and strongly polarised confirming this assignment. In CF_3Br, $\nu_3(e)$ is found at 350 cm^{-1}. The Se-Cl and Se-Br stretching modes, have been assigned to the bands at 367 and 255 cm^{-1} respectively in the molecules, Se_2Cl_2 and Se_2Br_2[55], and no separation has been observed between symmetric and asymmetric stretching modes. For our molecules, the bands appearing at 429 and 332 cm^{-1} appear to be suitable candidates for the Se-Cl (ν_5) and Se-Br (ν_5) stretching modes

respectively. The corresponding Raman band in both cases is of high intensity and polarised. The Se-Cl stretching mode shows a doublet structure in the Raman with a doublet separation of 6 cm^{-1}, which may be due to two isotopes of chlorine.

Aynsely et al.[54] have studied the infrared and Raman spectra of CH_3SeCN and assigned the three bands appearing at 2152, 384 and 365 cm^{-1} to C≡N stretching, SeC≡N in-plane (a') and out-of-plane (a") bending modes respectively. By analogy we have assigned the bands appearing at 2178, 396 and 354 cm^{-1} in the Raman spectrum of CF_3SeCN to C≡N stretching, in-plane and out-of-plane bending modes respectively. The lowest Raman bands at 129 and 118 cm^{-1} for CF_3SeCl and CF_3SeCN respectively are of medium intensity and depolarised and therefore theoretically should correspond to the torsional mode; the skeletal bending mode in CH_3SeCN is assigned to the polarised medium intensity band at 168 cm^{-1}. It is expected at still lower wavenumbers in our molecules, since the methyl group has been replaced by the heavier trifluoromethyl group. Thus it is more appropriate to assign the lowest Raman bands at 129 and 118 cm^{-1} to the skeletal bending modes, $\nu_8(a')$ and $\nu_{10}(a')$, of CF_3SeCl and CF_3SeCN respectively. The only difficulty with this assignment is that the bands are depolarised, whereas, theoretically they should be polarised. Similar anomalous behaviour has been observed earlier in the case of

$(CH_3)_2Se$[56] and $(CD_3)_2Se$[57], where the skeletal bending mode has been experimentally found to be depolarised. This has been explained there as follows:

The pure deformation modes should theoretically give rise to depolarisation ratios of slightly less than the maximum value of 6/7. Konigstein and Bernstein[58] have shown that depolarisation ratios of partly polarised lines may vary by as much as 10 per cent from the theoretical value, when effects of refractive index of the sample and intermolecular interactions are ignored as in the present case.

Thus a study of these compounds has more or less defined the regions for various vibrations of a CF_3Se group.

5.1.3 Bistrifluoromethyl Selenide

The molecule has been subjected to electron diffraction[47] and a C_2 symmetry proposed. The Raman spectrum shows only four polarised bands. Also the vibrational spectra resemble those of its methyl and perdeuteromethyl analogues[56,57], which have been analysed on the basis of a C_{2v} symmetry. Hence, a C_{2v} symmetry and zero angle of twist for the CF_3 groups is assumed. Figure 5 shows that the vibrational modes of a_1, b_1 and b_2 species should give B$\perp$, A$\parallel$ and C$\perp$ type band envelopes.

When a single CF_3 group is bonded to an atom of

atomic mass similar to that selenium (e.g. as in CF_3Br), vibrational modes of two species a_1 (symmetric) and e (doubly degenerate asymmetric) are observed. If now a second CF_3 group is attached to a heavy central atom, as in $(CF_3)_2Se$, two effects may become observable experimentally. First, the lower overall symmetry of the molecule should in principle

Molecular parameters: C-F = 1.334, C-Se = 1.975, $\angle FCF$ = 108.6 and $\angle CSeC$ = 97°.

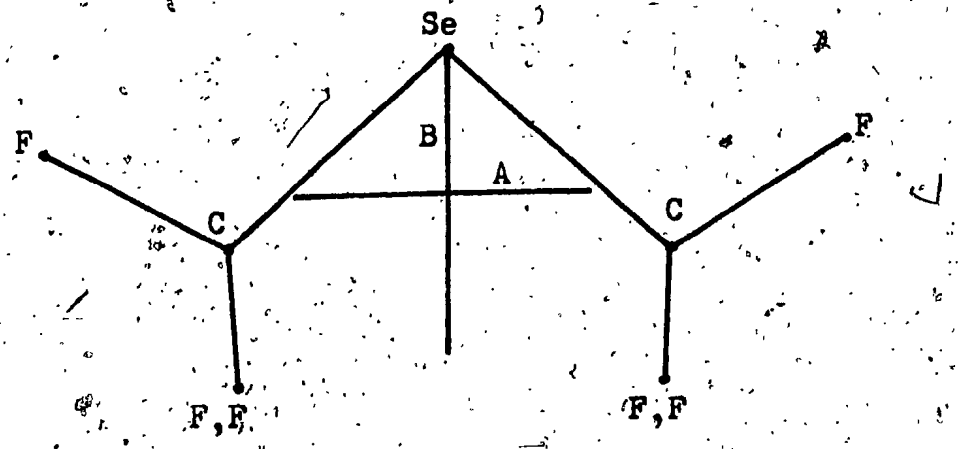

Figure 5. Projection of $(CF_3)_2Se$ in the C-Se-C plane along with the directions of inertial axes in this plane.

lift the degeneracy of asymmetric modes. Second, similar vibrational modes of each CF_3 group will interact with each other and in principle give rise to two modes one being symmetric and other asymmetric with respect to the plane perpendicular to C-Se-C plane of symmetry. These will be referred to as in-phase and out-of-phase modes of vibration. The amount

of splitting between these in- and out-of-phase modes is expected to be small as for $(CD_3)_2Se$[57]. For CF_3Br, two bands are observed in the C-F stretching region at approximately 1206 and 1085 cm^{-1}, the higher and lower wavenumber bands being assigned to asymmetric and symmetric stretching modes respectively. Taking above-mentioned arguments into consideration one should expect four bands around 1200 cm^{-1} and two bands around 1085 cm^{-1}. In fact only five bands are expected in the infrared as the a_2 modes are inactive, while all the six bands should appear in the Raman.

Three intense bands appear in the infrared at 1193, ≈ 1150 and 1065 cm^{-1} in the C-F stretching region. The bands at 1193 and ≈ 1050 cm^{-1} show a sub-band structure {Figure 8(a)} due to the overlapping of several bands. The intense infrared band at 1065 cm^{-1} which is depolarised in the Raman is assigned to $\nu_{13}(b_1)$, the out-of-phase C-F stretching mode whereas the 1142 cm^{-1} infrared band, which is weaker than the 1065 cm^{-1} band and polarised in the Raman is assigned to the corresponding in-phase mode $\nu_2(a_1)$. The nearly degenerate asymmetric C-F stretching modes of two CF_3 groups will interact with each other to give rise to four vibrational modes. The in-phase modes will belong to symmetry species a_1 and a_2 and out-of-phase to symmetry species b_1 and b_2. Out of these, the a_2 mode is inactive in the infrared and the remaining modes a_1,

b_1 and b_2 are expected to give B⊥ , A∥ and C⊥ type band contours respectively. Since a strong Q branch is observed at 1193 cm^{-1}, it is assigned to $\nu_{18}(b_2)$. The two bands at 1142 and 1152 cm^{-1} are too near to be of the same symmetry. Hence the 1152 cm^{-1} band is assigned $\nu_{12}(b_1)$. The remaining mode $\nu_1(a_1)$, is expected to give a B⊥ type band contour and is arbitrarily assigned to the first minimum of higher wavenumber band at 1193 cm^{-1}. $\nu_8(a_2)$ seems too weak to appear in the Raman, unless it is the depolarised band at 1178 cm^{-1}.

From considerations, similar to those given for the C-F stretching region, the CF_3 deformation region should also contain six bands in the Raman and five in the infrared spectrum. The six vibrational wavenumbers should again appear in two main groups. One group of two bands at around 750 cm^{-1} and another of four bands around 550 cm^{-1}, associated with symmetric and asymmetric deformation modes respectively. The two modes generated by the interaction of symmetric deformations belong to the symmetry species a_1 and b_1 and are expected to give band contours of B⊥ and A∥ type respectively. Only one strong band at 746 cm^{-1} is observed in the symmetric deformation region. The band shows a good PQR structure {Figure 8(a)} with a PR separation of 8.7 cm^{-1}, which agrees very well with the predicted value of 9.0 cm^{-1}, for an A∥ type band. Thus this band is assigned to $\nu_{14}(b_1)$, the out-of-

Molecule = $(CF_3)_2Se$ Symmetry type = C_{2v}

Number of genuine modes of vibration = 21

Symmetry species of the modes = $7a_1 + 4a_2 + 6b_1 + 4b_2$

Selection rules (for forbidden vibrations)

Infrared = ~~a_2, a_1~~ a_2, b_1 b_2, A_2^n (n = odd); Raman = none

Calculated principal moments of inertia (cm^{-1})

A = 0.0637, B = 0.0300, C = 0.0260

Calculated PR separations (cm^{-1}) and asymmetry parameters

A∥ = 9.0, B⊥ = 7.0, C⊥ = 13.4; κ = -0.78, $\rho^{\#}$ = 1.25

Table 8. Fundamental modes of $(CF_3)_2Se$, their assignments and expected band contour types.

Species	a_1			a_2			b_1			b_2		
Approximate description	Vib.	cm^{-1}	Band type	Vib.	cm^{-1}	Band type	Vib.	cm^{-1}	Band type	Vib.	cm^{-1}	Band type
C-F asym. str.	ν_1	1197	B⊥	ν_8	?		ν_{12}	1152	A∥	ν_{18}	1193	C⊥
C-F sym. str.	ν_2	1142	B⊥				ν_{13}	1065	A∥			
δ CF_3 sym.	ν_3	749	B⊥				ν_{14}	746	A∥			
δ CF_3 asym.	ν_4	538	B⊥	ν_9	553		ν_{15}	553	A∥	ν_{19}	535	C⊥
C-Se str.	ν_5	363	B⊥				ν_{16}	340	A∥			
CF_3 rock	ν_6	278	B⊥	ν_{10}	258		ν_{17}	253	A∥	ν_{20}	267	C⊥
C-Se-C bend	ν_7	109	B⊥									
CF_3 torsion				ν_{11}	?					ν_{21}	?	C⊥

Table 9. (Continued)

IR (gas)		Raman (liquid)			
pol.	cm^{-1}	cm^{-1}	pol.	I	Assignment
vs	1089				$\nu_{14} + \nu_{16} = 1086$
vs	1142	1133	p	vw	ν_2
vs	1152				ν_{12}
vs	1193 Q	1178	dp	vvw	ν_{18}
					ν_1
vs	1200				
vs	1206.5				
s	1278				$\nu_{14} + \nu_{19} = 1281$
w	1400				$\nu_2 + \nu_{10} = 1400$
w	1410				$\nu_2 + \nu_{20} = 1409$
vw	1465				$\nu_1 + \nu_{20} = 1464$
vw	1552				$\nu_5 + \nu_{18} = 1556$
vw	1560				$\nu_1 + \nu_5 = 1560$
vw	1678				
w	1712				$\nu_9 + \nu_{12} = 1705$
w	1816				$\nu_{13} + \nu_{14} = 1811$
w	1890				$\nu_2 + \nu_{14} = 1888$
w	1911				$\nu_3 + \nu_{18} = 1901$
vw	1944				$\nu_1 + \nu_3 = 1946$
vw	2137				$2\nu_{13} = 2130$

Table 9. Infrared and Raman spectra of $(CF_3)_2Se$

IR(gas)			Raman (liquid)			
pol.	cm^{-1}		cm^{-1}	pol.	I	Assignment
			109	dp	w	ν_7
vw	253					ν_{17}
			258	dp	w	ν_{10}
			267	?	?	ν_{20}
vw	278		278	p	vs	ν_6
m.	340		339	dp	w	ν_{16}
s	363		363	p	m	ν_5
w	528					
m	535	Q	537	dp	vw	ν_{19}
						ν_4
m	541					
			553	dp	vvw	ν_9, ν_{15}
w	614					$\nu_5 + \nu_{17} = 616$
w	700					$\nu_5 + \nu_{16} = 703$
vs	741.5	P				
	746	Q				ν_{14}
vs			749	p		ν_3
vs	750.2	R				
m	1025					$\nu_6 + \nu_{14} = 1024$
vs	1065		1056	dp	vvw	ν_{13}

Table 9. (Continued)

IR(gas)		Raman (liquid)			
pol.	cm^{-1}	cm^{-1}	pol.	I	Assignment
w	2206				$\nu_2 + \nu_{13} = 2207$
m	2235				
w	2294				$\nu_2 + \nu_{12} = 2294$
m	2336				$\nu_1 + \nu_2 = 2339$
w	2380				$2\nu_{18} = 2386$
w	2402				$2\nu_1 = 2394$

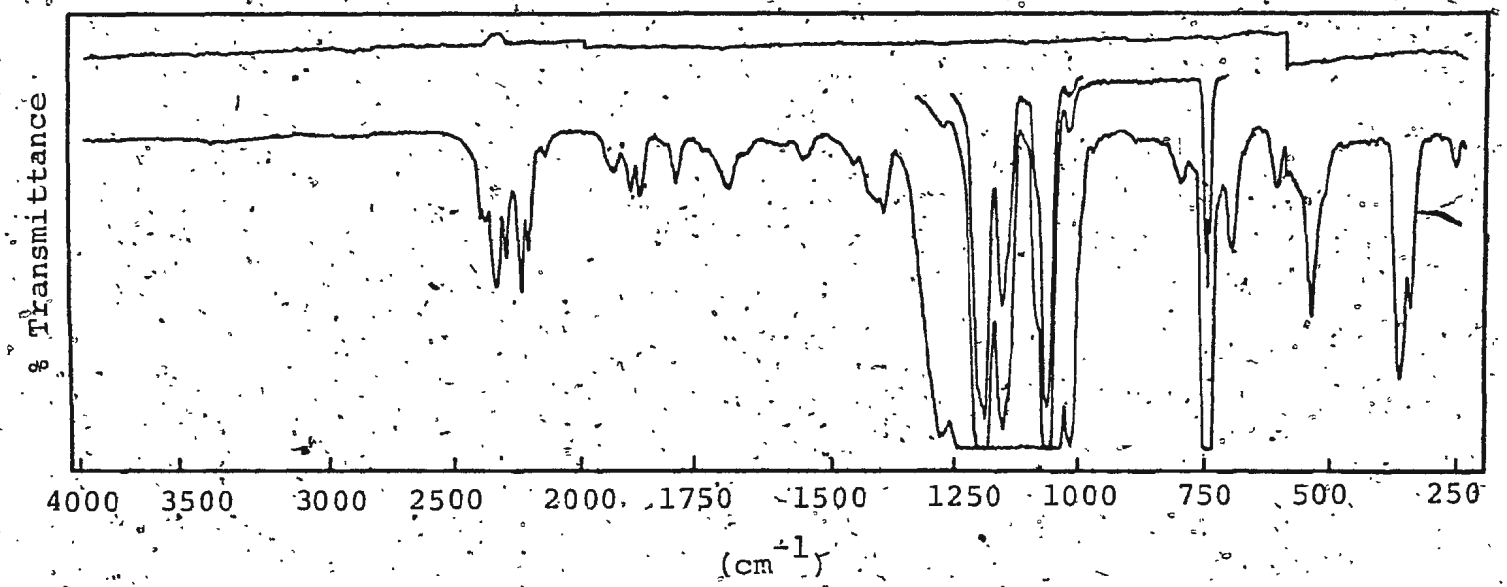

Figure 6. The gas phase infrared spectrum of $(CF_3)_2Se$.

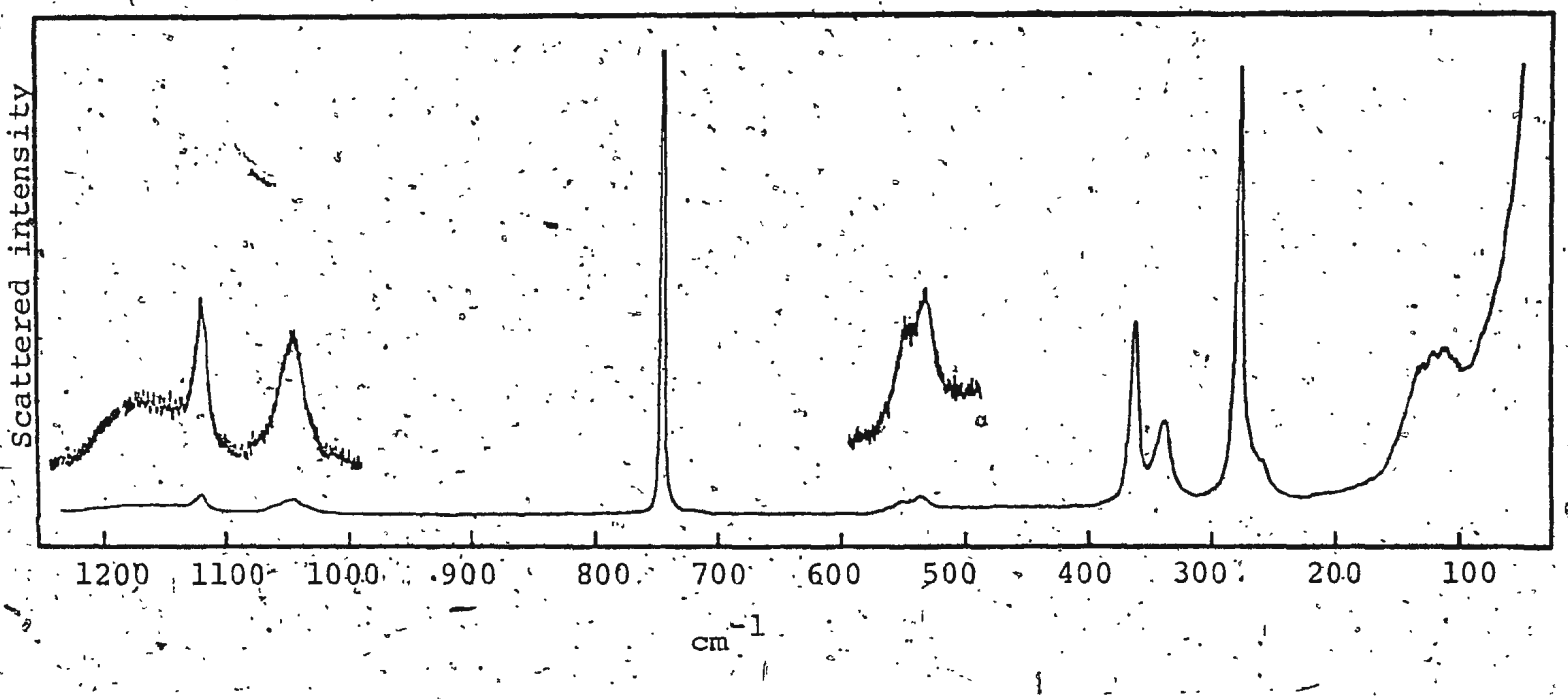

Figure 7. The liquid phase Raman spectrum of $(CF_3)_2Se$.

phase mode, while the intense Raman band at 749 cm^{-1} since it is strongly polarised should be assigned to the corresponding in-phase mode $\nu_3(a_1)$. Thus $\nu_{14}(b_1)$ is too weak to appear in the Raman, while $\nu_3(a_1)$ is too weak to appear in the infrared.

The four modes generated by the interaction of asymmetric deformations belong to the symmetry species a_1, b_1, a_2 and b_2. Out of these, the a_2 modes will be inactive in the infrared, while the remaining species are expected to give B⊥, A∥ and C⊥ type band envelopes respectively. Only one band is observed in the asymmetric deformation region in the infrared and has an intense Q branch at 535 cm^{-1}. The band shows a sub-band structure and is being overlapped on the higher wavenumber side by a B⊥ type band contour. Thus the first minimum on the higher wavenumber side is assigned to $\nu_4(a_1)$, while the Q branch at 535 cm^{-1} is ascribed to $\nu_{19}(b_2)$. The Raman band at 538 cm^{-1} is weak, broad and depolarised and hence corresponds to ν_{19}. The weak Raman band at 553 cm^{-1} has no infrared counterpart and therefore could be assigned to $\nu_9(b_2)$. $\nu_{15}(b_1)$ seems to be too weak to appear in the infrared, while in the Raman it may be hidden under $\nu_9(b_2)$.

Four rocking modes in total are expected and belong to symmetry species a_1, b_1, a_2 and b_2. Out of these, the a_2 mode is inactive in the infrared. Thus, four bands are

expected in the CF_3 rocking region in the Raman while only three bands are expected in the infrared. Only three bands appear in the Raman at 278 (p, vs), 267 (?, ?) and 258 (dp, w) cm^{-1} respectively, while only two bands are found in the infrared at 278 and 253 cm^{-1}. Assuming that the change in phase does not lead to any shift, four bands in total are observed. The highest wavenumber band is unambiguously assigned to $\nu_5(a_1)$, while out of the two remaining Raman bands one has to be assigned to the rocking mode, $\nu_{10}(a_2)$. Pending some more information (i.e. the observation of some more bands in the infrared etc.) it is not possible to make unambiguous assignments for the rocking modes. Thus the bands at 258, 267 and 253 cm^{-1} are tentatively assigned to the rocking modes $\nu_{10}(a_2)$, $\nu_{20}(b_2)$ and $\nu_{17}(b_1)$ respectively. For, if assigned this way, the assignments conform to the order of CH_3 rocking modes (cf. $a_1 > b_2 > a_2 > b_1$) observed in $Se(CH_3)_2$[56] and $Se(CD_3)_2$[57].

Coming to the vibrations of the C-Se-C skeleton, the previous study of the compounds, i.e. CF_3SeCl, CF_3SeBr and CF_3SeCN suggests that the C-Se stretching mode lies between 300 - 350 cm^{-1}. In the present molecule two bands are observed in the infrared at 363 and 340 cm^{-1}. The Raman band corresponding to the 363 cm^{-1} infrared band is of medium intensity and polarised. Therefore it is assigned to $\nu_5(a_1)$,

Figure 8.(a). Expanded scale gas-phase infrared spectra of some important fundamentals of CF_3SeCH_3, $(CF_3)_2Se$ and $(CF_3Se)_2$ in the region 1250 - 900 cm^{-1}.

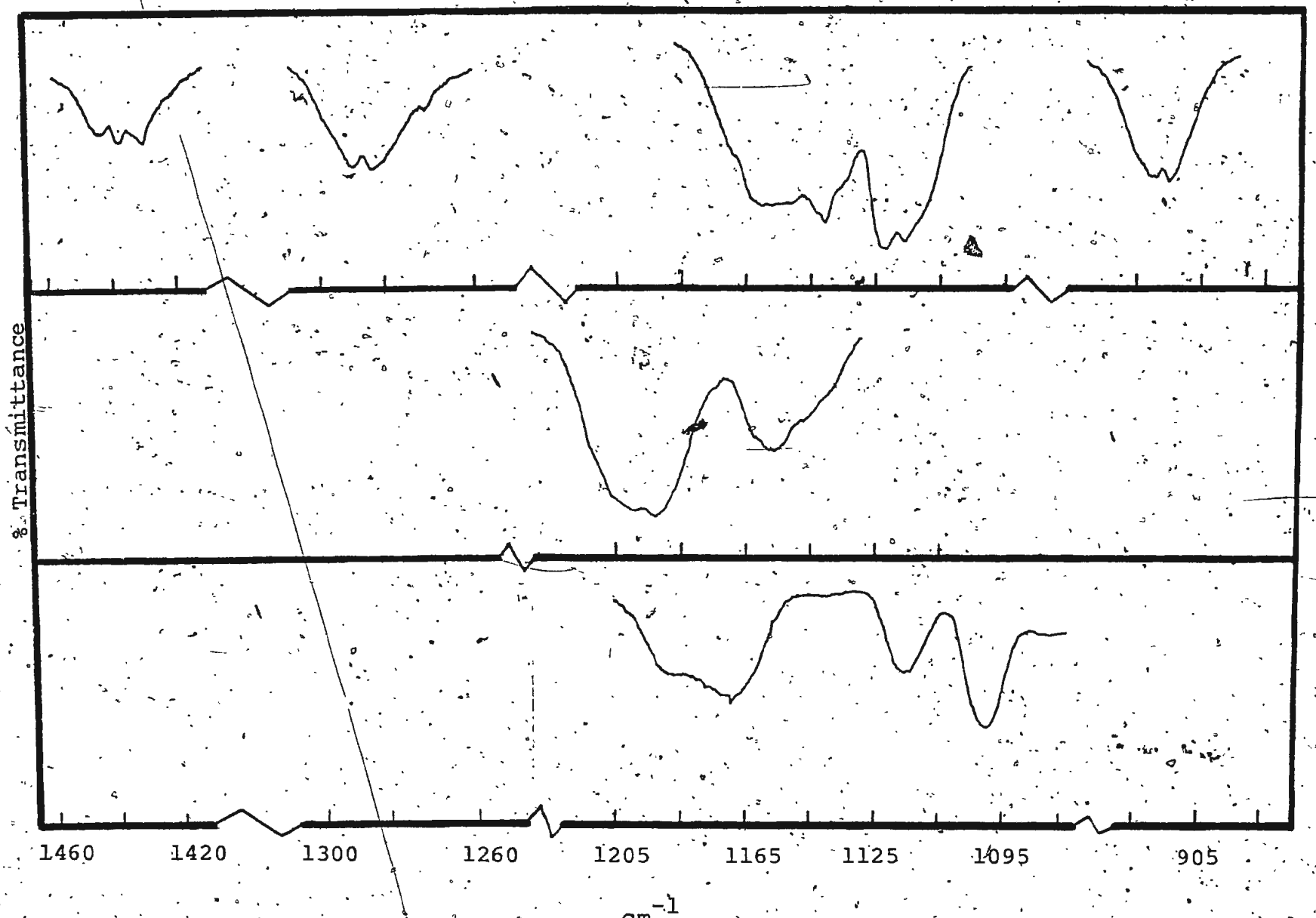
% Transmittance
1460
1420
1300
1260
1205
1165
1125
1095
905
cm-1

Figure 8 (a)

while the band corresponding to 340 cm^{-1} band is depolarised and of weak intensity and thus assigned to the C-Se-C asymmetric stretching mode, $\nu_{16}(b_1)$. Earlier studies on similar compounds, $Se(CH_3)_2$ [56] and $Se(CD_3)_2$ [57], show that the asymmetric C-Se stretching mode always lies at higher wavenumbers than the symmetric mode. The assignments are reverse in the present molecule. The reversal may be due to coupling between the C-Se stretching and CF_3 rocking modes in the present molecule. For the molecules $Se(CH_3)_2$ and $Se(CD_3)_2$, the lowest depolarised Raman band at 233 cm^{-1} and 201 cm^{-1} respectively has been assigned to the C-Se-C bending mode. Thus, the lowest band in the Raman at 109 cm^{-1} is assigned to $\nu_7(a_1)$, the C-Se-C bending mode. The band is again found to be depolarised, although theoretically it should be polarised. This discrepency has been explained on page 70.

5:1.4 Trifluoromethyl Methyl Selenide

The molecule will have C_s symmetry, if a zero angle of twist is assumed for the CF_3 and CH_3 groups. Twentyone normal modes of vibration are expected, out of which thirteen are symmetric (a') to the plane of symmetry, while eight are asymmetric (a"). It is obvious from Figure 9 that A and B axes lie near to the CF_3 and CH_3 group respectively. Thus, vibrational modes of the CF_3 group like symmetric stretch and deformation should show AB|| type band envelopes, while the

corresponding vibrational modes of the CH_3 group should show AB⊥ type band envelopes. Indeed, the infrared spectrum of the molecule testifies to this prediction.

The lowest band in the Raman at 148 cm^{-1} (depolarised) is assigned to the skeletal bending mode $\nu_{13}(a')$. The wavenumber of this mode has increased compared to the skeletal

Molecular parameters: C-F = 1.332, Se-C(F_3) = 1.984, C-H = 1.093, Se-C(H_3) = 1.943, ∠CSeC = 97, ∠FCF = 109.3 and ∠HCH = 110.2°.

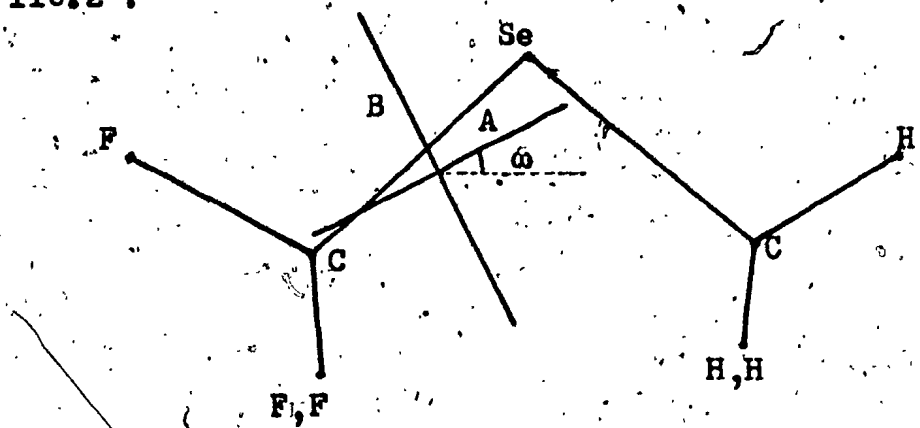

Figure 9. Projection of CF_3SeCH_3 in the plane of symmetry along with the directions of inertial axes in this plane.

bending mode in $(CF_3)_2Se$ because of the replacement of one heavier CF_3 group by the lighter CH_3 group. Next there are two Raman bands at 302 (m, dp) and 289 (w, dp) and they should be assigned to the two rocking modes $\nu_{12}(a')$ and $\nu_{19}(a'')$ respectively. The infrared spectrum in this region shows one

medium intensity band at 302 cm^{-1}. The band has PQR branches {Figure 8(b)} with PR separation of 10 cm^{-1}; which agrees well with the predicted value of 10.6 cm^{-1} for the AB|| type band. The other out-of-plane (a") rocking mode is too weak to be observed in the infrared. By comparison with other molecules studied in the earlier sections, the C-Se stretching mode $\nu_{11}(a')$ is assigned to the band at 340 cm^{-1}. The corresponding Raman band is polarised and strong as expected. The strong and strongly polarised Raman band at 593 cm^{-1} is assigned to $(H_3)C$-Se stretching mode $\nu_9(a')$. The symmetric and asymmetric C-Se-C stretching modes are observed in the Raman spectrum of $(CH_3)_2Se$ at 588 and 602 cm^{-1} respectively.

The spectrum in the CF_3 asymmetric deformation region is exactly similar to that of CF_3SeCl and CF_3SeBr, i.e. consisting of two overlapping bands. Thus, as before the midpoint of the band on higher wavenumber side is assigned to $\nu_{10}(a')$, while the lower wavenumber maximum at 533 cm^{-1} is assigned to the Q branch of $\nu_{18}(a")$, expected to give a C| type band contour. The corresponding Raman band is weak and depolarised confirming the assignment. The CF_3 symmetric deformation $\nu_8(a')$ is assigned to the band at 740 cm^{-1} and the band shows a good PQR structure {Figure 8(a)} with a PR separation of 12.2 cm^{-1}, which agrees with the predicted value of 11.3 cm^{-1} expected of an AB|| type band. The corres-

ponding Raman band is intense and strongly polarised.

Coming to the C-F stretching region two main bands are observed. As for the single CF_3 group containing molecules discussed earlier (sub-section 5.1.2) the higher wavenumber band consists of two overlapping bands. The band is quite broad on the higher wavenumber side because the moments of inertia for this molecule are smaller and therefore PR separations larger compared to other similar molecules (sub-section 5.1.2). The band is a composite of a' + a" modes of the otherwise degenerate CF_3 stretching mode. The mid-point of the higher wavenumber band is assigned to the mode $\nu_5(a')$, while the maximum at 1141 cm^{-1} (Q branch) represents $\nu_{16}(a")$, the out-of-plane asymmetric C-F stretching mode. The lower wavenumber band unlike other similar molecules does not show PQR structure but just a doublet, the Q branch is either missing or possibly overlaps the R branch. However, the corresponding Raman band is polarised supporting its assignment to the symmetric stretching mode, $\nu_6(a')$.

The assignments of the CH_3 group are straightforward. Three bands appear in the C-H stretching region both in infrared and Raman. The highest wavenumber band is weak and depolarised in the Raman. The band is assigned to a composite of C-H stretching modes $\nu_1(a')$ and $\nu_{14}(a")$, which are degenerate in CH_3Br. No splitting is observed

Molecule = CF_3SeCH_3

Calculated principal moments of inertia (cm^{-1})

A = 0.1236, B = 0.0582, C = 0.0505

Calculated PR separations (cm^{-1}) and asymmetry parameters

A∥ = 12.5, B⊥ = 9.7, C⊥ = 18.7; κ = -0.79, $\rho^{\#}$ = 1.29

Table 10. Fundamental modes of CF_3SeCH_3, their assignments and expected band contour types.

Species	a'			a"		
Approximate description	Vib.	cm^{-1}	Band type	Vib.	cm^{-1}	Band type
C-H asym. stretch	ν_1	3035	AB∥	ν_{14}	3035	C⊥
C-H sym. stretch	ν_2	2955	AB⊥			
CH_3 asym. deformation	ν_3	1441	AB∥	ν_{15}	1438	C⊥
CH_3 sym. deformation	ν_4	1292	AB⊥			
C-F asym. stretch	ν_5	1156	AB⊥	ν_{16}	1141	C⊥
C-F sym. stretch	ν_6	1117	AB∥			
CH_3 rock	ν_7	916	AB∥	ν_{17}	921	C⊥
CF_3 sym. deformation	ν_8	740	AB∥			
(H_3)C-Se stretch	ν_9	597	AB⊥			
CF_3 asym. deformation	ν_{10}	537	AB⊥	ν_{18}	533	C⊥
(F_3)C-Se stretch	ν_{11}	340	AB∥			
CF_3 rock	ν_{12}	302	AB⊥	ν_{19}	289	⊥
C-Se-C bend	ν_{13}	148	AB⊥			
CH_3 torsion				ν_{20}	?	C⊥
CF_3 torsion				ν_{21}	?	C⊥

Table 11. Infrared and Raman spectra of CF_3SeCH_3

IR(gas)			Raman (liquid)			
I	cm^{-1}		cm^{-1}	pol.	I	Assignment
			148	dp	w	ν_{13}
			289	dp	w	ν_{19}
m	296.5	P				
m	302	Q	302	p	m	ν_{12}
m	308.2	R				
s	340		339	p	ms	ν_{11}
vw	460					$\nu_{12} + \nu_{13} = 450$
w	533	Q	537	dp	vw	ν_{18}
						ν_{10}
w	540					
w	597		593	p	vs	ν_9
w	676		677	p	vvw	$2\nu_{11} = 680$
vs	733.8	P				
vs	740	Q	742	p	s	ν_8
vs	746	R				
vs	916	Q	911	p	vvw	ν_7
vs	921	Q				ν_{17}
m	1083		1079	p	vvw	$\nu_8 + \nu_{11} = 1080$
vs	1117	Q	1103	p	vw	ν_6
vs	1123	R				
vs	1134.7	R				

Table 11. (Continued)

IR(gas)			Raman (liquid)			
I	cm^{-1}		cm^{-1}	pol.	I	Assignment
vs	1141	Q				ν_{16}
vs	1156.5		1148	dp	vvw	
m	1272					$\nu_8 + \nu_{10} = 1277$
vs	1289		1292	p	vw	
vs	1294.5					ν_4
w	1333					
s	1431	P				
s	1438	Q	1432	dp	vw	ν_{15}
s	1444					ν_3
vw	1668					$\nu_{10} + \nu_{16} = 1674$
vw	1710					$\nu_6 + \nu_9 = 1714$
w	1869					$\nu_6 + \nu_8 = 1857$
w	1890					$\nu_4 + \nu_9 = 1899$
w	2208					$\nu_4 + \nu_7 = 2208$
w	2232					$2\nu_6 = 2234$
m	2250					$\nu_6 + \nu_{17} = 2358$
w	2272					$\nu_5 + \nu_6 = 2273$
w	2326					?
w	2851		2837	p	vw	$2\nu_{15} = 2876$
s	2955		2950	p	s	ν_2
w	3035		3031	dp	w	ν_1, ν_{14}

either in the infrared or in the Raman. The intermediate wavenumber band is intense and polarised. Thus, it is assigned to the symmetric stretching mode $\nu_2(a')$. The lowest wavenumber band is the first overtone of the asymmetric CH_3 deformation and is polarised. The triplet structure at 1438 cm^{-1} is assigned to the asymmetric deformations, with a' and a" components strongly overlapped. The first minimum on the higher wavenumber side is arbitrarily assigned to $\nu_3(a')$, while $\nu_{15}(a')$ is represented by the Q branch maximum at 1438 cm^{-1}. The corresponding Raman band at 1432 cm^{-1} is depolarised and of weak intensity. The strong doublet at ≈ 1292 cm^{-1} has a characteristic B⊥ type band envelope, because of the near proximity of the B axis and is assigned to $\nu_4(a')$, the symmetric CH_3 deformation mode. The corresponding Raman band at 1292 cm^{-1} is polarised confirming the assignment. The weak Raman band at 911 cm^{-1} is polarised and therefore assigned to the CH_3 rocking mode $\nu_7(a')$. The infrared spectrum in this region shows a doublet structure, with a doublet separation of 5 cm^{-1}. The lower wavenumber component of this doublet, at 916 cm^{-1}, perhaps corresponds to the Q branch of the in-plane rocking mode, $\nu_7(a')$, which is expected to give AB∥ type band contour. The higher wavenumber maximum at 921 cm^{-1} is ascribed to the Q branch of the out-of-plane mode, $\nu_{17}(a")$, which is expected to show a C⊥ type band contour.

5.1,5 Bistrifluoromethyl diselenide

The molecular structure of this molecule in vapor phase has been determined by electron diffraction[49] and found to be consistent with a C_2 model. The molecule has twenty-four normal modes of vibration, out of which thirteen are symmetric to the C_2 axis and hence belong to symmetry species a, while eleven modes are antisymmetric and therefore belong to the symmetry species b. All fundamentals and overtones are expected to be active in both infrared and Raman. From Figure 10 it is obvious that all a modes are expected to give B⊥ type band contours, while b modes should give AC hybrid type band envelopes. The molecule is made up of two equivalent CF_3Se groups bonded together through a Se-Se bond. Therefore the arguments of page 71 will also apply here, except that much less splitting is expected because of the insulating effect of the Se-Se bond.

Two strong bands, each with a sub-band structure {Figure 8(a)} are observed in the C-F stretching region. For the lower wavenumber band, the maximum at 1115 cm^{-1} is assigned to $\nu_3(a)$, the in-phase symmetric stretching mode, while the out-of-phase mode, $\nu_{16}(b)$, is assigned to the maximum at 1090 cm^{-1}. The Raman bands corresponding to the in- and out-of-phase modes are found to be polarised and depolarised respectively. For the higher wavenumber band, the maximum at

1188 cm^{-1} is arbitrarily assigned to $\nu_1(a)$ and $\nu_{14}(b)$, the first set of in- and out-of-phase components of nearly degenerate CF_3 asymmetric stretching modes. The maximum at

Molecular parameters: C-F = 1.326, C-Se = 2.018, Se-Se = 2.292 Å, /FCSe = 109.1, /C-Se-Se = 98° and dihedral angle = 84.5°.

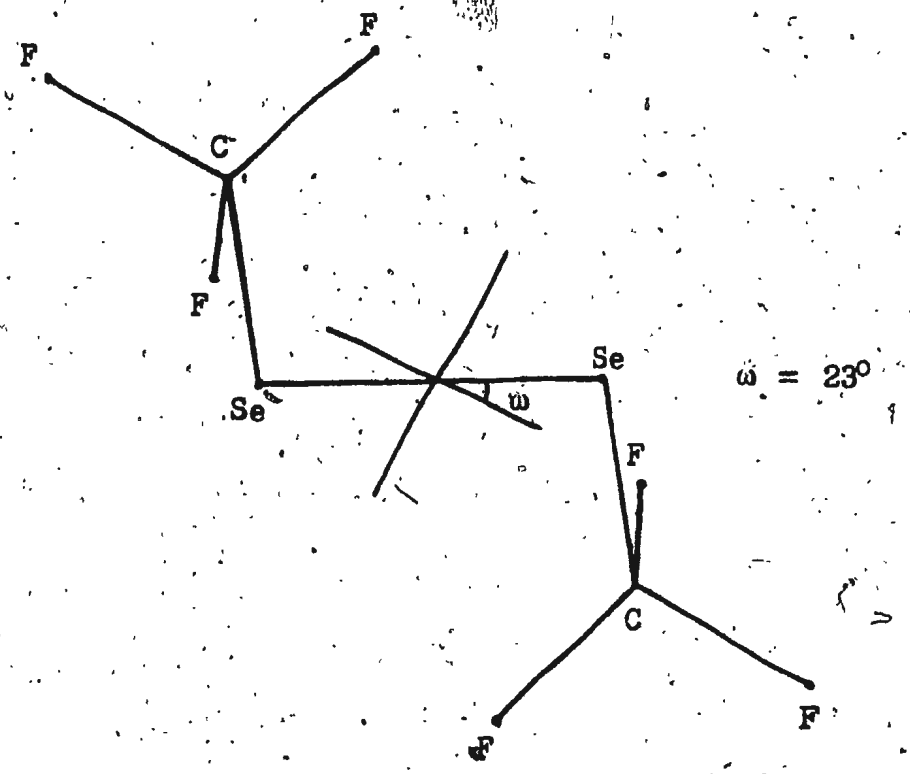

Figure 10. Projection of $(CF_3Se)_2$ in the plane perpendicular to C_2 axis along with the directions of inertial axes in this plane.

1169 cm^{-1} is then assigned to $\nu_2(a)$ and $\nu_{15}(b)$, the other set of in- and out-of-phase modes. The assignments for the higher wavenumber main band are tentative and could be reversed.

In the infrared, only one band at 741 cm^{-1} is observed in the CF_3 symmetric deformation region. The experimental PR separation of 6 cm^{-1} does not show a good agreement with the calculated value of 7.6 cm^{-1}. However, the band shows a PQR structure expected of an ACL type band contour. Therefore, the band is assigned to $\nu_{17}(b)$, the out-of-phase CF_3 deformation mode. The corresponding strong Raman band at 742 cm^{-1} is strongly polarised and is thus assigned to $\nu_4(a)$, the in-phase mode. The finding (pages 80 and 117) that for molecules containing two CF_3 groups, the in-phase CF_3 symmetric deformation mode is strong in the Raman whereas the out-of-phase mode is strong in the infrared also supports this assignment. In total four asymmetric CF_3 deformation modes are expected, i.e. two in-phase and two out-of-phase. Only one band is observed in the asymmetric CF_3 deformation region both in the infrared and Raman. Thus, some of the modes are either accidently degenerate or too weak to appear. Since a near degeneracy is observed between in- and out-of-phase symmetric CF_3 deformation modes, applying similar considerations to the asymmetric CF_3 deformation modes, the bands at 531 cm^{-1} could be easily assigned to the modes $\nu_6(a)$ and $\nu_{19}(b)$, while the weak and depolarised Raman band at 541 cm^{-1} could be assigned to the modes $\nu_5(a)$ and $\nu_{18}(b)$. The assignments are tentative and could be easily reversed.

Molecule = $(CF_3Se)_2$

Calculated principal moments of inertia (cm^{-1})

A = 0.0352, B = 0.0173, C = 0.0158

Calculated PR separations (cm^{-1}) and asymmetry parameters

$A_{\parallel}$ = 7.0, $B_{\perp}$ = 5.4, $C_{\perp}$ = 10.4; κ = -0.34, $\rho^{\#}$ = 1.12

Table 12. Fundamental modes of $(CF_3Se)_2$, their assignments and expected band contour types.

Species		a			b		
Approximate description	Vib.	cm^{-1}	Band type	Vib.	cm^{-1}	Band type
C-F stretch	ν_1	1188	B⊥	ν_{14}	1188	AC
	ν_2	1169	B⊥	ν_{15}	1169	AC
C-F sym. stretch	ν_3	1115	B⊥	ν_{16}	1090	AC
CF_3 sym. deformation	ν_4	742	B⊥	ν_{17}	741	AC
CF_3 asym. deformation	ν_5	541	B⊥	ν_{18}	541	AC
	ν_6	531	B⊥	ν_{19}	531	AC
C-Se stretch	ν_7	335	B⊥	ν_{20}	333	AC
CF_3 rock	ν_8	327	B⊥	ν_{21}	321	AC
	ν_9	280	B⊥	ν_{22}	287	AC
Se-Se stretch	ν_{10}	245	B⊥			
(F_3)C-Se-Se bend	ν_{11}	101	B⊥	ν_{23}	101	AC
CF_3 torsion	ν_{12}	?	B⊥			
Skeleton torsion	ν_{13}	?	B⊥			

Table 13. Infrared and Raman spectra of $(CF_3Se)_2$

IR(gas)		Raman (liquid)			
I	cm^{-1}	cm^{-1}	pol.	I	Assignment
		101	dp	s	ν_{11}, ν_{23}
		245	p	vs	ν_{10}
m	280				ν_9
		287	dp	w	ν_{22}
ms	321	318	dp	mw	ν_{21}
		327	?	?	ν_8
		333	p	s	ν_7, ν_{20}
vw	510				$\nu_9 + \nu_{10} = 525$
mw	531				ν_6, ν_{19}
		541	dp	w	ν_5, ν_{18}
vw	560				$2\nu_9 = 560$
vw	646				$2\nu_{21} = 642$
vs	738 P				
vs	741 Q				ν_{17}
		742	p	s	ν_4
vs	744 R				
w	1026				$\nu_{17} + \nu_{22} = 1028$
m	1072	1066	dp	vvw	$\nu_7 + \nu_{17} = 1076$
vs	1090	1084	dp	vvw	ν_{16}
vs	1115	1105	p	vw	ν_3
vw	1144				?

Table 13. (Continued)

IR (gas)		Raman (liquid)			
I	cm^{-1}	cm^{-1}	pol.	I	Assignment
vs	1169				ν_2, ν_{15}
vs	1188	1174	dp	vvw	ν_1, ν_{14}
s	1278				$\nu_5 + \nu_{17} = 1282$
vw	1715				$\nu_1 + \nu_5 = 1719$
vw	1736				$\nu_1 + \nu_6 = 1729$
vw	1836				$\nu_{16} + \nu_{17} = 1834$
w	1860				$\nu_3 + \nu_{17} = 1857$
w	1911				$\nu_2 + \nu_7 = 1910$
vw	1934				$\nu_1 + \nu_{17} = 1929$
vw	2184				$2\nu_{16} = 2180$
vw	2205				$\nu_3 + \nu_{16} = 2205$
vw	2236				$2\nu_3 = 2230$
w	2266				$\nu_2 + \nu_{16} = 2259$
w	2286				$\nu_2 + \nu_3 = 2284$
vw	2332				$2\nu_2 = 2338$
vw	2388				$2\nu_1 = 2376$

Br-Se-Se bending modes in Se_2Br_2 [59] have been assigned to the bands appearing at 107 and 115 cm^{-1}. Thus, the strong and depolarised lowest wavenumber band in the Raman at 101 cm^{-1} is assigned unambigously to the in- and out-of-phase $(F_3)C$-Se-Se bending modes $\nu_{11}(a)$ and $\nu_{23}(b)$. No splitting being observed in the liquid state.

We are now left with five unassigned bands in the Raman spectrum at 333 (p,s), 327 (??), 318 (dp,m), 287 (dp,m) and 245 (p, vs) cm^{-1} and two bands in the infrared at 321 (ms) and 280 (m) cm^{-1}. Apart from the torsional modes, there are seven unassigned vibrational modes, i.e. in- and out-of-phase C-Se stretch, Se-Se stretch and four CF_3 rocking modes. With the existing experimental data it is not possible to make unique assignments for some of these modes. The most probable set of assignments is discussed below.

Studies on the vibrational spectra of the analogous molecules Se_2Cl_2 [59], Se_2Br_2 [59], $Se_2(CH_3)_2$ [60] and other trifluoromethyl-selenium derivatives studies here have shown (i) Se-Se stretching mode occurs as a polarised, medium to very strong intensity band in the Raman at 280 cm^{-1}, (ii) Se-Se stretch is a good group wavenumber which shows a medium-weak intensity band in the infrared, (iii) C-Se stretching modes give a medium to strong intensity band between 325-350 cm^{-1} and no splitting has been observed between the

in- and out-of-phase C-Se stretching modes, (iv) CF_3 rocking modes are in general quite weak in the infrared.

According to criterion (iv), the infrared bands at 321 and 280 cm^{-1}, which are of medium intensity, could not be the rocking modes and perhaps correspond to the Raman bands at 327 and 287 cm^{-1} respectively. The apparent shift is assumed to be a reflection of the change in phase. Thus the Raman bands at 333 and 327 cm^{-1} are assigned to the in-, and out-of-phase C-Se stretching modes respectively. The band at 287 cm^{-1}, although depolarised, can be assigned to Se-Se stretching vibration. The other two left out Raman bands could then be assigned to the CF_3 rocking modes. Bomford[9] has also assigned the Raman band at 287 cm^{-1} to the Se-Se stretch. The above assignments suffer from the defect that Se-Se stretch is observed to be depolarised and of weak intensity, whereas it is expected to be strong and polarised.

5.2 The Phosphorus Compounds

5.2.1 General

Though the earlier studies cited in the introduction, the region for the internal vibrations of trifluoromethyl-group has been identified to be more or less the same as for the selenium compounds. The region for P-C stretching modes has been identified to be 425 - 475 cm^{-1}, which is quite low when compared to the region of P-C stretching modes in methylphosphines (675 - 725 cm^{-1}). The low wavenumber of the P-C stretching modes in perfluoromethyl compounds could be attributed to the longer P-C bond[50] and heavier CF_3 group (P-C bond in $P(CF_3)_3$ = 1.937Å compared to 1.87Å in $P(CH_3)_3$). The CF_3 rocking modes have been mostly observed between 100 - 250 cm^{-1}. Thus, these earlier studies have helped in the interpretation of the vibrational spectra of the compounds reported in subsequent pages. The compounds are being discussed in the order of increasing complexity. The first compound, CF_3PF_2, contains just one CF_3 group and only two bands are observed in the C-F stretching region. The next compound, $(CF_3)_2PF$, contains two CF_3 groups and a slight crowding occurs. For the last compound, $P(CF_3)_3$, there are three CF_3 groups and hence the C-F stretching region is very much crowded. Also, the Raman depolarisation ratios are of

no use as all bands in the C-F stretching region are weak and appear to be depolarised. Thus, one can give only tentative assignments for C-F stretching modes. Nevertheless, the infrared band contours study helped in making unambiguous assignments for many C-F stretching and other modes.

Very recently, Bürger et al.[23] have reported with assignments the infrared and Raman spectra of $(CF_3)_3P/As/Sb$. Their assignments are based upon normal co-ordinate analysis. The assignments of Bürger et al., which do not agree with ours will be criticised in the proper sections. The infrared bands which show some structure are shown in Figure 13. All compounds, except $P(CF_3)_3$, are prolate asymmetric rotors and are shown in Figures 11 and 12.

5.2.2 Trifluoromethyldifluorophosphine

If the CF_3 group is oriented in such a way that one of the fluorine atoms is locked in the plane of symmetry, the molecule will belong to the C_s point group and the spectra have been analysed on the basis of this symmetry. It is obvious from Figure 11 that all in-plane (a') and out-of-plane (a") modes should produce AC hybrid- and B⊥ type band contours respectively.

Two strong bands appear in the C-F stretching region at 1222 and 1160 cm^{-1}. In the infrared the higher wavenumber band is weaker than the lower wavenumber band,

while in the Raman the reverse is the case. Thus, the higher wavenumber band is assigned to $\nu_1(a')$, the symmetric stretching mode, while the lower wavenumber band is assigned to a composite of $\nu_2(a')$ and $\nu_{10}(a'')$, the nearly degenerate asymmetric stretching modes. It seems that the local symmetry of the CF_3 group is over-riding the lower C_s overall symmetry.

Molecular parameters: C-F = 1.342, C-P = 1.937, P...F = 2.715, P-F = 1.535Å and $\angle CPC = \angle CPF = \angle FPF = 99.6^\circ$.

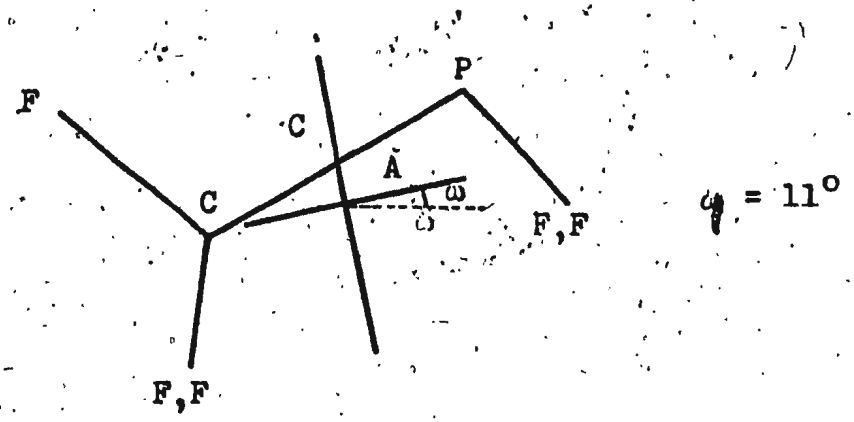

Figure 11. Projection of CF_3PF_2 in the plane of symmetry along with the directions of inertial axes in this plane.

Earlier studies on similar molecules: CF_3PCl_2[17], CF_3PH_2[18] and CF_3AsCl_2[19] have shown that the symmetric stretching mode lies above the asymmetric stretching mode. Berney[61] has collected data on a large number of CF_3 compounds and shown, when the trifluoromethyl group is attached to only one atom (e.g. CF_3Br), the asymmetric

stretching mode lies above the symmetric mode, but when the trifluoromethyl group is attached to the carbon of a polyatomic group, the reversal of the order occurs. Also, the study of the next member, $(CF_3)_2PF$, confirms it to some extent. The infrared band contours and the Raman depolarisation ratios in this region cannot be put to any use as both the bands appear to be featureless and depolarised.

The symmetric CF_3 deformation mode, $\nu_4(a')$, is assigned to the weak band at 748 cm^{-1}. The corresponding Raman band is strongly polarised confirming this assignment. Next, two bands are observed at 558 and 564 cm^{-1}, while only one depolarised band is observed in the Raman at 567 cm^{-1}. The infrared doublet cannot be correlated to a B⊥ type band contour as the doublet separation is less than expected of a B⊥ type band. A close look at the band contour shows a slight kink at 552 cm^{-1}. So the first minimum at 561 cm^{-1} can be assigned to $\nu_{12}(a'')$, the out-of-plane component of the otherwise degenerate asymmetric deformation, while the maximum at 558 cm^{-1} is assigned to the Q branch of AC⊥ type band contour expected from the corresponding in-plane component, $\nu_5(a')$.

As for the vibrations of the PC_2F skeleton, the replacement of one of the fluorine atoms in PF_3 by a dissimilar atom or group splits the doubly generate stretching

mode into a' and a" modes, referred to as symmetric and antisymmetric P-F stretch respectively. The degenerate mode occurs at 860 cm^{-1} in PF_3. One very important point to be observed in the compounds[62,63]: PF_3, $ClPF_2$ and $BrPF_2$ is that as the electronegativity of the odd atom decreases the splitting between symmetric and asymmetric P-F stretching modes also decreases. Also, the symmetric stretching mode is always found to lie at higher wavenumbers than the asymmetric one. The difference is 12 cm^{-1} in $ClPF_2$, 9 cm^{-1} in $BrPF_2$ and should still decrease slightly for the present molecule and this is the reason that on crossing the polariser, the Raman band maximum at 863 cm^{-1} shifts to about 7 cm^{-1} lower. Thus, the Raman band at 863 cm^{-1} consists of two overlapping bands and the higher wavenumber component is polarised. The infrared band corresponding to the 863 cm^{-1} Raman band shows a PQR structure (Figure 13), expected of an AC$\|$ type band and therefore is assigned to $\nu_3(a')$, the symmetric PF_2 stretching mode. The observed PR separation of 12 cm^{-1} does not agree with the predicted value of 16.8 cm^{-1}. Perhaps the structure is a composite of a' + a" modes, which show a coriolis coupling. The Raman band at 859 cm^{-1} is assigned to $\nu_{11}(a")$, the asymmetric PF_2 stretching mode.

The P-C stretching mode, $\nu_6(a')$, is assigned to the band at 463 cm^{-1}. The band is at much lower wavenumbers

Molecule = CF_3PF_2 Symmetry type = C_s

Number of normal modes of vibration = 15

Symmetry species of the modes = 9a' + 6a"

Selection rules (for forbidden vibration)

Infrared = none; Raman = none

Calculated principal moments of inertia (cm^{-1})

A = 0.1107, B = 0.0595, C = 0.0517

Calculated PR separations (cm^{-1}) and asymmetry parameters

A∥ = 12.8 B⊥ = 9.8 C⊥ = 19.3; κ = -0.74 $\rho^{\#}$ = 0.99

Table 14. Fundamental modes of CF_3PF_2, their assignments and expected band contour types.

Species		a'			a"		
Approximate description		Vib.	cm^{-1}	Band type	Vib.	cm^{-1}	Band type
C-F sym. stretch		ν_1	1222	A∥	?		
C-F asym. stretch		ν_2	1160	A⊥	ν_{10}	1160	B⊥
P-F stretch		ν_3	863	A⊥	ν_{11}	856	B⊥
CF_3 sym. deformation		ν_4	748	A∥			
CF_3 asym. deformation		ν_5	558	A⊥	ν_{12}	561	B⊥
P-C stretch		ν_6	463	A∥			
PF_2 bend		ν_7	388	A⊥			
PF_2 way		ν_8	280	A∥			
PF_2 twist					ν_{13}	325	B⊥
CF_3 rock		ν_9	199	A⊥	ν_{14}	106	B⊥
CF_3 torsion					ν_{15}	?	

Table 15. Infrared and Raman spectra of CF_3PF_2

IR(gas)			Raman (liquid)			
I	cm^{-1}		cm^{-1}	pol.	I	Assignment
			106	p	w	ν_{14}
			199	dp	w	ν_9
			242	p	vvw	?
w	280		282	p	s	ν_8
vw	325		323	dp	w	ν_{13}
m	380	P				
m	388	Q	386	p	s	ν_7
m	395	R				
w	433					$\nu_{13} + \nu_{14} = 431$
ms	456.5	P				
s	463	Q	461	p	m	ν_6
ms	470	R				
m	552					
ms	558					ν_5
			567	dp	w	ν_{12}
ms	564					
vw	596					$\nu_7 + \nu_9 = 587$
vw	604					$\nu_8 + \nu_{13} = 605$
vw	748		746	p	vs	ν_4
vs	860		856	dp	w	ν_{11}
vs	865		863	p	m	ν_3

Table 15. (Continued)

IR(gas)		Raman (liquid)			
I	cm^{-1}	cm^{-1}	pol.	I	Assignment
vs	870.5				
w	918				$2\nu_6 = 927$
mw	1035				$\nu_6 + \nu_{12} = 1024$
w	1062				$\nu_3 + \nu_9 = 1062$
vs	1156.5				
vs	1160	1159	?	vw	ν_2, ν_{10}
vs	1217				
vs	1222	1223	?	w	ν_1
m	1285				$\nu_2 + \nu_{14} = 1266$
m	1307				$\nu_4 + \nu_5 = 1306$
w	1356				$\nu_2 + \nu_9 = 1359$
m	1723				$2\nu_3 = 1726$
w	1900				$\nu_2 + \nu_4 = 1908$
vw	1962				$\nu_1 + \nu_4 = 1960$
w	2305				$2\nu_2 = 2320$
w	2387				$\nu_1 + \nu_2 = 2382$
w	2436				$2\nu_1 = 2444$

than 692 cm^{-1}, for the stretching mode in CH_3PCl_2 (17). The low value is justified because the C-Br stretching mode is assigned a value of 348 cm^{-1} in CF_3Br as opposed to a value of 611 cm^{-1} in CH_3Br. The band at 463 cm^{-1} shows a PQR structure. The observed PR separation of 13.5 cm^{-1} shows a good agreement with the predicted value of 15 cm^{-1}, expected of an ACII type band.

The replacement of one of the fluorine atoms in PF_3 by a dissimilar atom or group also splits the degenerate bending modes into two modes a' and a". However, now this a" and the a' mode formed from the a' mode in PF_3 constitute the asymmetric and symmetric bending modes, called the PF_2 twist and wag respectively. Thus now the a' mode of e mode in PF_3 called the PF_2 bending mode remains fixed with respect to the molecule, while the other two modes twist and wag become mostly the characteristic of the odd atom. Except the torsional mode, five modes now remain to be assigned, three of which belong to the symmetry species a' and hence should give polarised bands. Six bands are observed in the Raman spectrum at 386 (p, s), 323 (dp, w), 282 (p, s), 242 (p, vvw), 199 (dp, w) and 106 (p, w) cm^{-1}. The 242 cm^{-1} band is too weak to be assigned to a fundamental. The band at 386 cm^{-1} is unambiguously assigned to the PF_2 bending mode, $\nu_7(a')$. The corresponding infrared band is of medium intensity and

shows a PQR structure with a PR separation of 15 cm^{-1}, while the predicted value for an AC⊥ band is 16.8 cm^{-1}. Assuming rocking modes to lie below 250 cm^{-1}, as has been found in many trifluoromethyl- phosphorus/arsenic compounds cited earlier, the bands at 199 and 106 cm^{-1} are assigned to rocking modes, $\nu_{14}(a")$ and $\nu_9(a')$, respectively. The bands at 323 and 282 cm^{-1} are then assigned to the PF_2 twisting and wagging modes, $\nu_{13}(a")$ and $\nu_8(a')$ respectively. The only weak point against this assignment is that PF_2 twisting mode lies above the wagging mode, whereas generally for molecules of type YPF_2[63] (Y = Cl, Br), the reverse is found to be the case.

For assigning the skeletal modes, the CF_3PF_2 molecule can be considered equivalent to $BrPF_2$[63], where the CF_3 group has been replaced by an equally massive bromine atom. In this molecule, the bands at 391, 233 and 112 cm^{-1} have been assigned to PF_2 bending, wagging and twisting modes respectively. Thus, the bands at 199 and 106 cm^{-1} should be assigned to PF_2 wagging and twisting modes respectively. The rocking modes then correspond to the bands at 323 and 282 cm^{-1} respectively. If this set of assignments were to be correct the 106 cm^{-1} band should have been depolarised, while it is found to be polarised.

5.2.3 Bistrifluoromethylfluorophosphine

This molecule differs from the earlier molecule in

that one more fluorine atom has been replaced by a CF_3 group; it most probably belongs to the C_s symmetry. The molecule has twenty-four active fundamentals, of which thirteen belong to the symmetry species, a', while eleven fundamentals belong to the symmetry species, a". All fundamentals and overtones are active both in the infrared and Raman. From Figure 12 it is obvious that all in-plane (a') vibrations are expected to

Molecular parameters: C-F = 1.342, C-P = 1.937, P...F = 2.715, P-F = 1.535 Å and $\angle CPC = \angle CPF = \angle FPF = 99.6^{\circ}$.

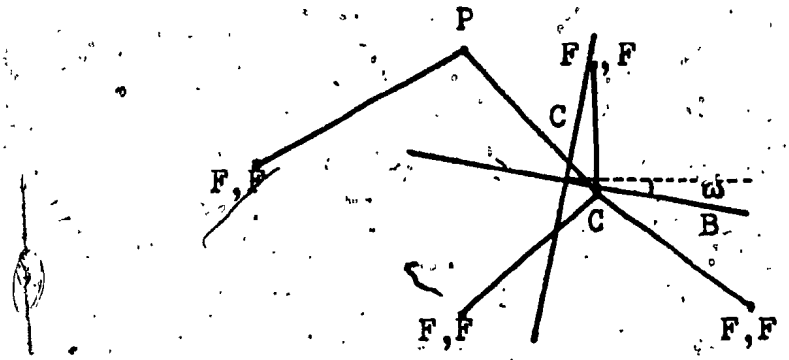

Figure 12. Projection of $(CF_3)_2PF$ in the plane of symmetry along with the directions of inertial axes in this plane.

show BC hybrid type bands, while all out-of-plane vibrations are expected to give A|| type band contours.

Since there are two CF_3 groups bonded to a central phosphorus atom, applying considerations similar to those

given on Page 71 (for $(CF_3)_2Se$) and assuming a weak mechanical interaction one would expect two bands near the symmetric stretching mode and a cluster of four bands near the asymmetric stretching mode of a single CF_3 group. Three main bands are present in the C-F stretching region. The lowest band shows a sub-band structure with four peaks at 1151.5, 1146, 1138 and 1133.5 cm^{-1} respectively. The Raman band corresponding to the 1179 cm^{-1} infrared bands seems to be polarised and is therefore assigned to $\nu_1(a')$, the in-phase symmetric stretching mode. The band at 1229 cm^{-1} is assigned to the corresponding out-of-phase mode $\nu_{14}(a'')$. The sub-band structure between 1151.5 and 1133.5 cm^{-1} (Figure 13) seems to be formed by the strong overlapping of the four bands. The first minimum on the higher wave number side is assigned to $\nu_2(a')$, which should give a BC|| type band contour; this is strongly overlapped by the A|| type contour of $\nu_{15}(a'')$ with Q branch at 1146 cm^{-1}. The peak maximum at 1138 cm^{-1} is assigned to the Q branch of $\nu_3(a')$, which, if $\nu_2(a')$ has BC|| type band contour, should have BC⊥ type band contour. The last maximum at 1133.5 cm^{-1} is correlated with the Q branch of A|| type band contour expected out of $\nu_{16}(a'')$. The Bürger et al.[23] assignments for $P(CF_3)_3$ seem to suggest that for a single CF_3 group attached to phosphorus the asymmetric stretching mode lies above the symmetric stretching mode. If true, the observed sub-band structure at the lower

Molecule = $(CF_3)_2PF$

Calculated moments of inertia (cm^{-1})

A = 0.0593, B = 0.0293, C = 0.0255

Calculated PR separations (cm^{-1}) and asymmetry parameters

$A_{||}$ = 9.3, $B_{\perp}$ = 6.9, $C_{\perp}$ = 13.4; κ = -0.77, $\rho^{\#}$ = 1.15

Table 16. Fundamental modes of $P(CF_3)_2F$, their assignments and expected band contour types.

Species	a'			a"		
Approximate description	Vib.	cm^{-1}	Band type	Vib.	cm^{-1}	Band type
C-F sym. stretch	ν_1	1179	BC$_{\|\|}$	ν_{14}	1229	A$_{\|\|}$
C-F asym. stretch	ν_2	1151.5	BC	ν_{15}	1146	A$_{\|\|}$
	ν_3	1138	BC	ν_{16}	1133.5	A$_{\|\|}$
P-F stretch	ν_4	852	BC$_{\|\|}$			
CF_3 sym. deformation	ν_5	748	BC$_{\|\|}$	ν_{17}	754	A$_{\|\|}$
CF_3 asym. deformation	ν_6	573	BC	ν_{18}		A$_{\|\|}$
	ν_7	543	BC	ν_{19}		A$_{\|\|}$
P-C stretch	ν_8	457	BC$_{\|\|}$	ν_{20}		A$_{\|\|}$
PC_2 wag	ν_9	354	BC$_{\perp}$			
PC_2 bend	ν_{10}	275	BC$_{\|\|}$			
PC_2 twist				ν_{21}	238	A$_{\|\|}$
CF_3 rock	ν_{11}	189	BC	ν_{22}	184	A$_{\|\|}$
	ν_{12}	118	BC	ν_{23}	112	A$_{\|\|}$
CF_3 torsion	ν_{13}	?		ν_{24}	?	A$_{\|\|}$

Table 17. Infrared and Raman spectra of $P(CF_3)_2F$

IR(gas) I	IR(gas) cm^{-1}		Raman (liquid) cm^{-1}	Raman (liquid) pol.	Raman (liquid) I	Assignment
			112	?	vw	ν_{23}
			118	p	w	ν_{12}
			184	?	vvw	ν_{22}
			189	p	vw	ν_{11}
m	235		238	dp	mw	ν_{21}
mw	275		275	p	vs	ν_{10}
m	354		354	p	m	ν_9
vw	426					$\nu_1 - \nu_{17} = 425$
s	457		456	p	m	ν_8
w	479					$\nu_{14} - \nu_{17} = 475$
w	518		527	dp	vw	$\nu_{17} - \nu_{21} = 516$
mw	543		545	dp	w	ν_7, ν_{19}
ms	573		569	dp	w	ν_6, ν_{18}
vw	727		733	p	vvw	$\nu_6 + \nu_{11} = 732$
			748	p	vs	ν_5
w	749.5	P				
mw	754	Q				ν_{17}
w	759	R				
vs	852		850	p	m	ν_4
w	912					$2\nu_8 = 914$
vw	983					$\nu_{17} + \nu_{21} = 992$

Table 17. (Continued)

IR(gas)		Raman (liquid)			
I	cm^{-1}	cm^{-1}	pol.	I	Assignment
w	1029				$\nu_6 + \nu_8 = 1030$
m	1092				$\nu_4 + \nu_{21} = 1088$
vs	1133.5	1122	?	vw	ν_{16}
vs	1138				ν_3
vs	1146	1140	?	vw	ν_{15}
vs	1151.5				ν_2
vs	1179	1169	?	vw	ν_1
vw	1206				$\nu_8 + \nu_{17} = 1211$
vs	1229	1226		vvw	ν_{14}
s	1274				$\nu_2 + \nu_{12} = 1269.5$
s	1298				$\nu_6 + \nu_{17} = 1297$
w	1360				$\nu_1 + \nu_{22} = 1363$
w	1403				$\nu_{10} + \nu_{16} = 1408.5$
vw	1452				$\nu_1 + \nu_{10} = 1454$
vw	1500				$\nu_2 + \nu_9 = 1505.5$
w	1698				$\nu_6 + \nu_{16} = 1706.5$
vw	1722				$\nu_2 + \nu_6 = 1724.5$
vw	1800				$\nu_6 + \nu_{14} = 1802$
w	1884				$\nu_{16} + \nu_{17} = 1887.5$
w	1929				$\nu_1 + \nu_5 = 1933$

Table 17. (Continued)

IR(gas)		Raman (liquid)			
I	cm^{-1}	cm^{-1}	pol.	I	Assignment
vw	1978				$\nu_{14} + \nu_{17} = 1983$
m	2278				$\nu_{15} + \nu_{16} = 2279.5$
vw	2311				$\nu_1 + \nu_{16} = 2312.5$
w	2348				$2\nu_1 = 2358$
vw	2412				$\nu_1 + \nu_{14} = 2408$
w	2454				$2\nu_{14} = 2458$

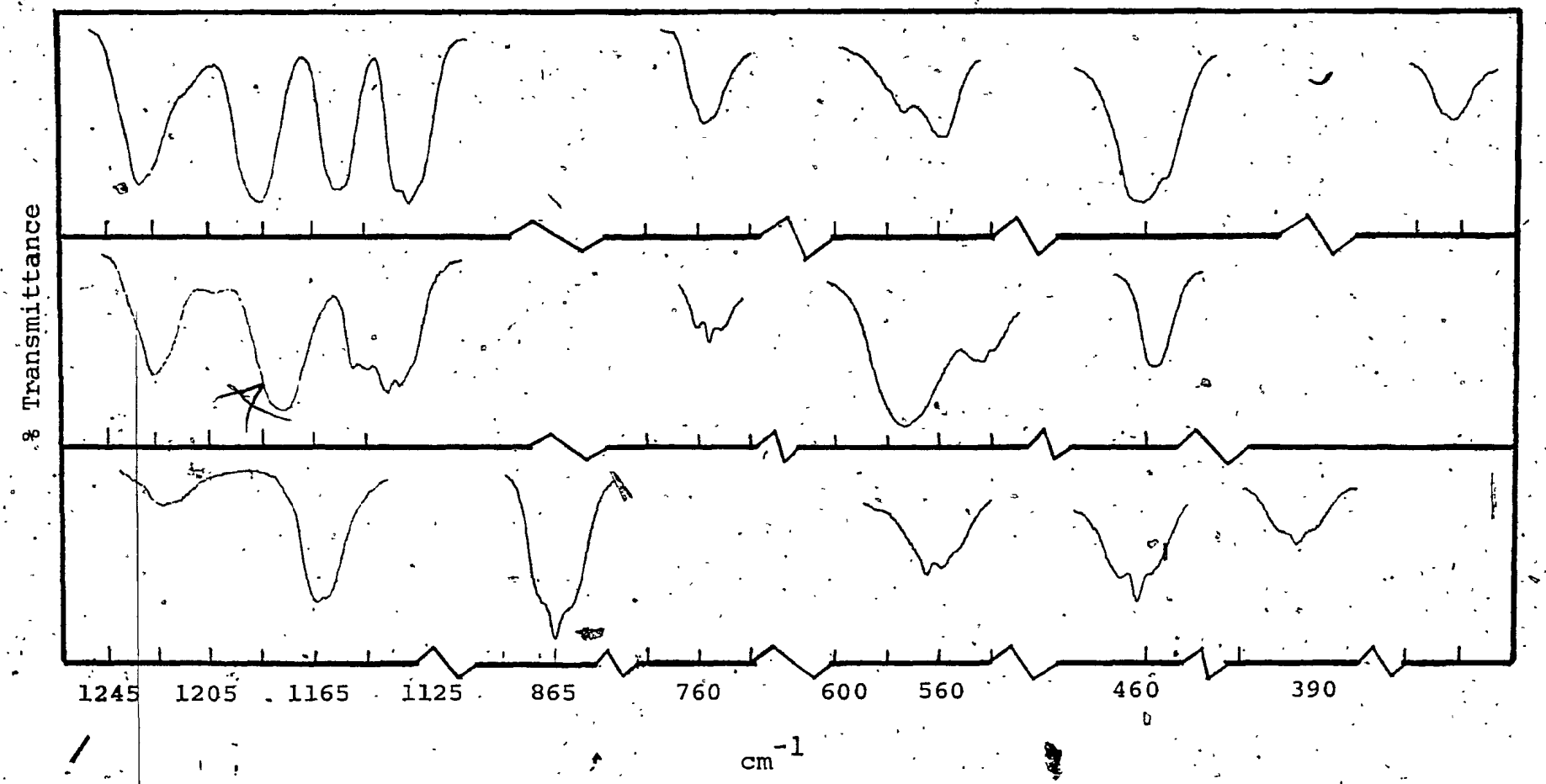

Figure 13. Expanded scale gas phase infrared spectra of $(CF_3)_3P$, $(CF_3)_2PF$ and CF_3PF_2 in the region 1250 - 250 cm^{-1}.

wavenumber end cannot be explained. Thus, the study of infrared band contours has been useful in making the assignments less ambiguous.

The medium intensity band at 754 cm^{-1} shows a PQR structure (Figure 13) with a PR separation of 9.5 cm^{-1} expected of an A|| band and hence should correspond to $\nu_{17}(a'')$, the out-of-phase deformation mode, $\nu_{17}(a'')$, while the corresponding in-phase mode is assigned to the strongly polarised Raman band at 748 cm^{-1}. Thus the in- and out-of-phase modes are nearly degenerate with the out-of-phase mode more intense in the infrared and the in-phase mode more intense in the Raman. The asymmetric CF_3 deformation region shows two bands at 573 and 543 cm^{-1} respectively. The Raman spectrum also shows two bands at 545 and 569 cm^{-1}. Both bands are weak and depolarised. If one assumes that there is no splitting between the in- and out-of-phase modes (as is true for symmetric deformation modes), the band at 573 cm^{-1} can be assigned to the asymmetric deformation modes, $\nu_6(a')$ and $\nu_{18}(a'')$, while the band at 543 cm^{-1} is assigned to $\nu_7(a')$ and $\nu_{19}(a'')$ modes. These assignments are tentative and could be easily reversed.

For the vibrational modes of the PC_2F skeleton, the P-F stretching mode $\nu_4(a')$ is assigned unambiguously to the strong band at 852 cm^{-1}. In the P-C stretching region

only one strong band is observed at 457 cm^{-1}. The corresponding Raman band at 456 cm^{-1} is not strongly polarised suggesting both $\nu_8(a')$ and $\nu_{20}(a'')$ to be accidentally degenerate. Apart from the torsional modes, the seven remaining fundamentals are to be assigned to five main Raman bands. Since in similar molecules: CF_3PCl_2[17], $(CF_3)_2AsCl$[19] and CF_3AsCl_2[19] etc. the rocking modes have been found to lie at lower wavenumbers than the skeletal modes, the Raman bands at 354 (p, m), 275 (p, vs) and 238 (dp, mw) are assigned to $\nu_9(a')$, $\nu_{10}(a')$ and $\nu_{21}(a'')$, the PC_2 wagging, bending and twisting modes respectively. Each of the two lowest wavenumber bands at 189 and 118 cm^{-1} seems to possess a sub-band structure with weaker components at - 184 and - 112 cm^{-1}. It is not possible to determine their depolarisation ratios, but the main bands are definitely polarised. Thus the bands at 189 and - 184 cm^{-1} are assigned to the rocking modes $\nu_{11}(a')$ and $\nu_{22}(a'')$ respectively, while the rocking modes, $\nu_{12}(a'')$ and $\nu_{23}(a'')$, are ascribed to the bands at 118 and 112 cm^{-1} respectively. Thus, there exists little splitting between the in- and out-of-phase rocking modes. The assignments of the rocking modes are tentative and could be easily reversed.

The skeletal modes of this molecule could also be assigned by comparison with the equivalent molecule Br_2PF[63],

obtained by replacing the CF_3 groups with equally massive bromine atoms. For this molecule the bands at 258, 220 and 126 cm^{-1} have been assigned to PBr_2 wagging, twisting and bending modes respectively. Thus for the present molecule, the bands at 275, 238 and 118 cm^{-1} could be assigned to PC_2 wagging, twisting and bending modes respectively. The bands at 189 and 354 cm^{-1} then remain to be assigned to the four rocking modes. This set of assignments will also satisfy Bürger et al.[23], who have found the rocking modes to lie above the skeletal bending modes in $P(CF_3)_3$. But this second set of assignments cannot explain the sub-band structure observed for the two lowest Raman bands.

5.2.4 Tristrifluoromethylphosphine

The electron diffraction studies[50] have shown that this molecule has a pyramidal structure similar to trimethylphosphine except that the P-C bonds are a little longer. Both the PC_3 framework and CF_3 groups have a local symmetry of C_{3v}, but the entire molecule has a C_{3v} symmetry for only two unique sets of positions of the CF_3 groups about their ternary axis. The infrared and Raman spectra shows that the vibrations of the PC_3 framework and CF_3 rocking modes can be interpreted in terms of a local C_{3v} symmetry in which the perfluoromethyl groups are considered to be cylindrically symmetric. Also, the vibrations of CF_3

groups, i.e. stretching and deformation modes, can be discussed in terms of a local and overall C_{3v} symmetry.

The molecule has thirty-three normal modes of vibration, which for a C_{3v} symmetry group to give twenty-two distinguishable modes. Seven belong to the symmetry species a_1 four to a_2 and eleven to species e. The a_1 modes are infrared active and Raman polarised. The a_2 modes are inactive both in the infrared and Raman and the e modes are infrared active and Raman depolarised. The principal moments of inertia have been calculated and show the molecule to be oblate symmetric rotor.

The five normal modes of the C-F stretching vibrations can be imagined to be constructed from symmetric and asymmetric vibrational modes of each CF_3 group. Thus the three symmetric modes, one from each CF_3 group will interact with each other to produce one in-phase (totally symmetric) and one out-of-phase (doubly degenerate) mode. The amount of splitting between the in- and out-of-phase modes will depend on the mechanical coupling and probably is not large. Similarly the degenerate asymmetric modes of each CF_3 group will interact with each other to generate one in-phase (totally symmetric) and two out-of-phase (degenerate) modes.

Four strong infrared bands are observed in the C-F stretching region at 1128, 1155, 1186 and 1231 cm^{-1}.

The lowest wavenumber band shows a PQR structure expected of a C|| type band with a PR separation of 9 cm^{-1}, which agrees well with the predicted value of 9.8 cm^{-1}. Hence this band should be assigned to an a_1 mode, although the corresponding Raman band at 1122 cm^{-1} is slightly if at all polarised. In the molecule $(CF_3)_2PF$, discussed earlier, the symmetric stretching mode is found to lie above the asymmetric stretching mode; assuming the same to be true in the present molecule, one can assign the band at 1128 cm^{-1} to $\nu_2(a_1)$, the in-phase asymmetric stretching mode, while the bands at 1186 and 1155 cm^{-1} are assigned to the corresponding out-of-phase modes $\nu_{13}(e)$ and $\nu_{14}(e)$. The band at 1231 cm^{-1} is ascribed to $\nu_{12}(e)$, the out-of-phase symmetric C-F stretching mode, while the corresponding in-phase mode, ν_1, is ascribed to the Raman band at 1192 cm^{-1}, which appears to be depolarised because of the proximity of a depolarised band at 1179 cm^{-1}. These assignments although fully compatible with the experimental data are only tentative.

The deformation modes may also be considered to be formed in a manner similar to the C-F stretching modes. Therefore, two bands are expected in the CF_3 symmetric deformation region, while four bands are expected to form a cluster in the asymmetric CF_3 deformation region. The infrared band at 753 cm^{-1} seems to be a perpendicular band

Molecule = $P(CF_3)_3$

Calculated principal moments of inertia

A = 0.0255, B = 0.0255, C = 0.0162

Calculated PR separations (cm^{-1}) and asymmetry parameters

$\parallel$ band = 9.8, $\perp$ band = 7.8; $\kappa = 1$, $\rho^{\#} = 0.37$

Table 18. Fundamental modes of $P(CF_3)_3$, their assignments and expected band contour types.

Species	a_1			a_2			e		
Approximate description	Vib.	cm^{-1}	Band type	Vib.	cm^{-1}	Band type	Vib.	cm^{-1}	Band type
C-F sym. stretch	ν_1	1192	$\parallel$				ν_{12}	1231	$\perp$
C-F asym. stretch	ν_2	1128	$\parallel$	ν_8			ν_{13}	1186	$\perp$
							ν_{14}	1155	$\perp$
CF_3 sym. deformation	ν_3	748	$\parallel$				ν_{15}	753	$\perp$
CF_3 asym. deformation	ν_4	574	$\parallel$	ν_9			ν_{16}	559	$\perp$
							ν_{17}	532	$\perp$
P-C stretch	ν_5	453	$\parallel$				ν_{18}	462.5	$\perp$
PC_3 deformation	ν_6	270	$\parallel$				ν_{19}	286	$\perp$
CF_3 rock	ν_7	150	$\parallel$	ν_{10}			ν_{20}	246	$\perp$
							ν_{21}	112	$\perp$
CF_3 torsion		?		ν_{11}			ν_{22}	?	$\perp$

Table 19. Infrared and Raman spectra of $P(CF_3)_3$

IR(gas)			Raman (liquid)			
I	cm^{-1}		cm^{-1}	pol.	I	Assignment
			112	dp	w	ν_{21}
			150	p	vw	ν_7
w	246	Q	251	dp	w	ν_{20}
w	250	R				
			270	p	vs	ν_6
			286	dp	m	ν_{19}
s	453		452	p	ms	ν_5
s	462.5		464	dp	m	ν_{18}
vw	532		532	dp	vw	ν_{17}
m	559		558	dp	vw	ν_{16}
m	574		571	dp	w	ν_4
w	727		722	p	vvw	$\nu_5 + \nu_6 = 723$
w	749.5		748	p	vs	ν_3
m	753	Q	753	?	w?	ν_{15}
vw	818					$\nu_{17} + \nu_{19} = 818$
vw	863					$\nu_4 + \nu_{19} = 861$
vw	925					$2\nu_{18} = 925$
vw	997					$\nu_{17} + \nu_{18} = 994.5$
w	1026					$\nu_6 + \nu_{15} = 1025$
vw	1040					$\nu_{15} + \nu_{19} = 1039$

Table 19. (Continued)

IR(gas)			Raman (liquid)			
I	cm^{-1}		cm^{-1}	pol.	I	Assignment
vs	1124	P	1120	p?	vw	
vs	1128	Q				ν_2
vs	1133	R				
vs	1155					ν_{14}
vs	1186		1179	?	vvw	ν_{13}
			1192	?	vvw	ν_1
w	1220					$\nu_{15} + \nu_{18} = 1215.5$
vs	1231		1234	?	vvw	ν_{12}
w	1285					$\nu_{15} + \nu_{17} = 1285$
w	1315					$\nu_{15} + \nu_{16} = 1312$
w	1352					$\nu_{12} + \nu_{21} = 1343$
vw	1378					$\nu_7 + \nu_{12} = 1381$
vw	1416					$\nu_2 + \nu_{19} = 1414$
vw	1430					$\nu_{13} + \nu_{20} = 1432$
vw	1652					$\nu_2 + \nu_{17} = 1660$
vw	1680					$\nu_{14} + \nu_{17} = 1687$
vw	1713					$\nu_{13} + \nu_{17} = 1718$
vw	1722					$\nu_4 + \nu_{14} = 1726$
vw	1798					$\nu_4 + \nu_{12} = 1802$
vw	1878					$\nu_2 + \nu_{15} = 1881$

Table 19. (Continued)

IR(gas)		Raman (liquid)			
I	cm^{-1}	cm^{-1}	pol.	I	Assignment
vw	1909				$\nu_{14} + \nu_{15} = 1913$
vw	1936				$\nu_{13} + \nu_{15} = 1939$
vw	1976				$\nu_{12} + \nu_{15} = 1984$
mw	2248				$2\nu_2 = 2256$
vw	2280				$\nu_{12} + \nu_{14} = 2386$
w	2308				$2\nu_{14} = 2310$
vw	2338				$\nu_{13} + \nu_{14} = 2341$

and is being overlapped on the lower wavenumber side (shown by the kink at 749.5) by the parallel type band of the in-phase mode. The corresponding intense Raman band is also made up of two components, for with a crossed polariser a clear doublet appears. The lower wavenumber component at 748 cm^{-1} is strong and definitely polarised. The depolarisation ratio of the higher wavenumber component is difficult to measure. Thus the Raman bands at 748 and 753 cm^{-1} are assigned to $\nu_{14}(a)$ and $\nu_{15}(e)$, the in-phase and out-of-phase asymmetric deformation modes. Three bands are observed both in the infrared and Raman in the asymmetric deformation region. The highest wavenumber band since it is polarised in the Raman is assigned to $\nu_4(a_1)$, the in-phase asymmetric deformation mode, while the other two bands at 559 and 532 cm^{-1} are assigned to the two out-of-phase modes $\nu_{16}(e)$ and $\nu_{17}(e)$. The assignments for $\nu_{16}(e)$ and $\nu_{17}(e)$ are tentative and could be easily reversed.

As for the PC_3 skeletal modes, by comparison among themselves and other trifluoromethylphosphorus compounds cited earlier, the medium intensity bands at 462.5 and 453 cm^{-1} can be assigned unambiguously to the P-C stretching modes. The higher wavenumber band being depolarised is assigned to the mode $\nu_{18}(e)$, while the polarised low wavenumber band is ascribed to the mode $\nu_5(a_1)$. For the molecule

$As(CF_3)_3$[19], the skeletal modes have been found to lie in the same region as the bending modes in $As(CH_3)_3$. Trimethylphosphine[64] exhibits its a_1 and e skeletal bending modes at 263 and 305 cm^{-1} respectively. The skeletal bending modes in the present molecule are thus expected to have similar wavenumbers. Thus the Raman bands at 286 and 270 cm^{-1} are assigned to the bending modes $\nu_{19}(e)$ and $\nu_6(a_1)$ respectively. The higher wavenumber band is of medium intensity and depolarised, while the lower wavenumber band is strong and polarised.

Earlier studies on similar compounds (cited in introduction) have shown CF_3 rocking modes to lie at relatively low wavenumbers (i.e. 100 - 250 cm^{-1}). Four rocking modes in total are expected, of which the a_2 mode is inactive in both infrared and Raman. Thus, only three rocking modes are to be observed and the Raman spectrum indeed shows three bands in this region at 251, 150 and 112 cm^{-1}. The band at 150 cm^{-1} is polarised and therefore assigned to $\nu_7(a_1)$, the totally symmetric in-phase rocking mode, while the 150 and 112 cm^{-1} bands, which are depolarised, are assigned to $\nu_{20}(e)$ and $\nu_{21}(e)$ respectively, the out-of-phase rocking modes.

Very recently Bürger et al.[23] have reported with assignments the infrared and Raman spectra of $(CF_3)_3P/As/Sb$. Their assignments are based upon the normal co-ordinate

analysis. Their reported spectra of $P(CF_3)_3$ agree quite well with ours except for one or two bands. However, their assignments for the CF_3 rocking and stretching modes do not agree with ours, which are mainly based upon the study of infrared band contours, Raman depolarisation ratios and analogies among themselves and with other compounds studied by Griffiths and others and cited earlier. Bürger et al. have shown that the rocking modes in the molecule $P(CF_3)_3$ lie above the skeletal bending modes. Thus they have assigned the bands at 286, 270 and 251 cm^{-1} to the three rocking modes, while the bands at 150 and 112 cm^{-1} are assigned to the doubly degenerate and non-degenerate PC_3 bending modes respectively. If their assignments were correct the lowest band should be polarised, while it is observed to be depolarised. Also, if in closely related molecules, CF_3PF_2 and $(CF_3)_2PF$, the CF_3 rocking modes are assumed to lie above the bending modes, certain difficulties are experienced (page 109 and 119) in making assignments compatible with the experimental data. As well, for the molecule $P(CF_3)_3$, assignments of Bürger et al. do not agree with ours in the C-F stretching region. Their assignments seem to suggest that for a single CF_3 group bonded to phosphorus, the symmetric C-F stretching modes lie below the asymmetric C-F stretching mode, while our study seems to suggest that reverse is true.

5.3 Conclusions

The C-F stretching modes have been found to give very strong bands in the infrared, while in the Raman they give weak and broad bands. For selenium compounds, the symmetric C-F stretching mode always lies below the asymmetric stretching mode, while the reverse has been found to be the case with phosphorus compounds. For selenium compounds containing a single CF_3 group, the symmetric C-F stretch in general shows a perturbed PQR structure and slight splitting has been observed between a' and a" components of the asymmetric C-F stretching mode. For compounds containing two or more CF_3 groups, the in- and out-of-phase C-F stretching modes show some splitting.

The CF_3 symmetric deformation mode is a good group wavenumber and is always found around 745 cm^{-1} and remains constant to $\pm$ 6 cm^{-1} over both phosphorus and selenium compounds. For all compounds, except CF_3PF_2 and $(CF_3)_3P$, this mode always shows PQR structure. For selenium compounds containing one CF_3 group, the CF_3 symmetric deformation mode is always found to be very strong in both infrared and Raman, while for CF_3PF_2 it is weak in the infrared and strong in the Raman. For compounds containing two or more CF_3 groups, the out-of-phase CF_3 deformation mode is strong in the infrared and weak in the Raman, while reverse is the case for the in-

phase mode. Only a negligible splitting is observed between these in- and out-of-phase modes. The infrared band contour study has very much helped in establishing this important observation. The asymmetric deformation modes occur in the region 530 - 575 cm^{-1}. The degeneracy of this mode seems to be slightly lifted in the molecules of low symmetry (i.e. C_s). However, no splitting has been observed between the in- and out-of-phase asymmetric deformation modes.

The $(F_3)C$-Se stretching modes in general give medium to strong intensity infrared bands. The bands show PQR structure only for CF_3SeCN and CF_3SeCH_3. The corresponding Raman band is always strong. These vibrational modes are found in the region 315 - 350 cm^{-1}. P-C stretching modes also behave as good group wavenumbers and are always found around 460 cm^{-1} and remain constant within ± 3 cm^{-1}. This mode shows a PQR structure only in the case of CF_3PF_2. No splitting has been observed between the symmetric and asymmetric P-C stretching modes in $(CF_3)_2PF$. The P-F stretching modes are confined within 10 cm^{-1} and occur as very strong bands in the infrared, while in the Raman they give bands of medium intensity. In the case of CF_3PF_2 a little splitting is observed between the symmetric and asymmetric P-F stretching modes. The splitting is consistent with the available data on compounds $ClPF_2$ and $BrPF_2$ (page 104).

The CF_3 rocking modes (which are degenerate in CF_3Br and CF_3Cl) show the greatest splitting. For the selenium and phosphorus compounds these modes are found between 250 - 300 and 100 - 250 cm^{-1} respectively. For the selenium compounds these modes are found to be weak in the infrared, while in the Raman the modes generally give weak to medium intensity bands. In general not much splitting has observed between the in- and out-of-phase rocking modes.

LITERATURE CITED

1. F.W. Bennett, H.J. Emeléus and R.N. Haszeldine, J. Chem. Soc., 1565 (1953).
2. J.W. Dale, H.J. Emeléus and R.N. Haszeldine, J. Chem. Soc., 2939 (1958).
3. H.J. Emeléus and M.J. Dunn, J. Inorg. Nucl. Chem., 27, 752 (1965).
4. N.N. Yarovenko, V.N. Shemanina and G.B. Gazieva, Zhur. Obschei Khim., 29, 942 (1959).
5. W.F. Edgell and C.E. May, J. Chem. Phys., 22, 1808 (1954).
6. W.F. Edgell and R. Potter, J. Chem. Phys., 24, 80 (1956).
7. S.N. Nabi and N. Sheppard, J. Chem. Soc. 3439 (1959)
8. H.J. Clase, Ph. D. thesis, The University of Cambridge, (1963).
9. D.R.L. Bomford, M.Sc. thesis, The University of Sussex (1968).
10. M.A.A. Beg and H.C. Clark, Can. J. Chem., 40, 393 (1962)
11. A.B. Burg and J.E. Griffiths, J. Am. Chem. Soc., 84, 3442 (1962).
12. J.E. Griffiths, Spectrochim. Acta, 24A, 115 (1968)
13. J.E. Griffiths, Spectrochim. Acta, 24A, 303 (1968)
14. J.E. Griffiths, J. Chem. Phys., 49, 1307 (1968).
15. J.E. Griffiths and A.L. Beach, J. Chem. Phys., 44, 2686 (1966).

16. J.E. Griffiths, J. Chem. Phys., 41, 3510 (1964).

17. J.E. Griffiths, Spectrochim. Acta, 21, 1135 (1965).

18. L.J. Anthony, Ph.D. thesis, The University of Pennsylvania (1966).

19. L.N. Craft, Ph.D. thesis, The University of Wisconsin (1965).

20. R.H. Atalla and A.D. Craig, J. Chem. Phys., 45, 423 (1966).

21. R.H. Atalla and A.D. Craig, J. Chem. Phys., 45, 427 (1966).

22. P.J. Hendra, R.A. Johns, C.T.S. Miles, C.J. Vear and A.B. Burg, Spectrochim. Acta, 26A, 2169 (1970).

23. H. Burger, J. Cichon, J. Grobe and F. Hofler, Spectrochim. Acta, 28A, 1275 (1972).

24. J.F. Nixon, J. Chem. Soc., A, 1136 (1967).

25. J.F. Nixon and M.D. Sexton, Inorg. Nucl. Chem. Lett. 4, 275 (1968).

26. J.F. Nixon and M.D. Sexton, J. Chem. Soc. A, 1089 (1969).

27. C.G. Barlow, J.F. Nixon and M. Webster, J. Chem. Soc. A, 2216 (1968).

28. R. Schmutzler, Amer. Chem. Soc. Advances in chemistry series, No. 37, 150 (1963).

29. I.P. Komkov, S.Z. Ivin, K.W. Karawanov and L. Smirnov, Zhur. Obschei Khim., 32, 301 (1962).

30. R. Schmutzler, Inorg. Chem., 3, 410 (1964).

31. J.O. Hirschfelder, J. Chem. Phys., 8, 431 (1940)

32. Joint Commission for Spectroscopy, J. Chem. Phys., 23, 1997 (1955).

33. S.L. Gerhard and D.M. Dennison, Phys. Rev., 43, 197 (1933).

34. W.A. Seth-Paul and G. Dijkstra, Spectrochim. Acta, 23A, 2861 (1967).

35. J.M. Hollas, Spectrochim. Acta, 22, 81 (1966).

36. R.M. Badger and L.R. Zumwalt, J. Chem. Phys., 6, 711 (1938).

37. W.A. Seth-Paul, J. Mol. Structure, 3, 403 (1969).

38. W.A. Seth-Paul, and H.J. De-Meyer, J. Mol. Structure, 3, 11 (1969).

39. H.J. Emeléus and N. Welchman, J. Chem. Soc., 1268 (1963).

40. A.B. Burg and G. Brendel, J. Am. Chem. Soc., 80, 3198 (1958).

41. A.B. Burg and G. Brendel, U.S. Patent no. 2,959, 620 (Nov. 8, 1960).

42. J.F. Nixon, J. Chem. Soc., 2469 (1964).

43. V.N. Kulakova, Yu. M. Zinovev and L. Soborovski, Zhur. Obschei Khim., 29, 3957 (1959).

44. International union of pure and applied chemistry, commission on molecular structure and spectroscopy "Tables of wavenumbers for the calibration of infrared spectrometers", Butterworths, London (1961).

45. L.R. Blaine, E.K. Plyer and W.S. Benedict, J. Res. NBS. A Phys. Chem. 66A, 223 (1962).

46. Massachusetts Institute of Technology wavelength tables, the M.I.T. press, Cambridge, Massachusetts.

47. C.J. Marsden and G.M. Sheldrick, J. Mol. Structure, 10, 405 (1971).

48. C.J. Marsden and G.M. Sheldrick, J. Mol. Structure, 10, 413 (1971).

49. C.J. Marsden and G.M. Sheldrick, J. Mol. Structure, 10, 419 (1971).

50. H.J.M. Bowen, Trans. Faraday Soc., 50, 463 (1954).

51. J.F. Beecher, J. Mol. Spectrosc., 21, 414 (1966).

52. E. Hirota, Bull. Chem. Soc. Japan, 31, 130 (1958).

53. Handbook of Chemistry and Physics 51st edition.

54. E.E. Aynsely, N.N. Greenwood and M.J. Sprague, J. Chem. Soc., 2395 (1965).

55. R. Forneris and C.E. Hennies, J. Mol. Structure, 5, 449 (1920).

56. J.R. Allkins and P.J. Hendra, Spectrochim. Acta, 22, 2075 (1966).

57. J.R. Allkins and P.J. Hendra, Spectrochim. Acta, 23A, 1671 (1967).

58. J.A. Koningstein and H.J. Bernstein, Spectrochim. Acta, 18, 1249 (1962).

59. P.J. Hendra and P.J.D. Park, J. Chem. Soc. A, 908 (1968).

60. S.G. Frankiss, J. Mol. Structure, 3, 89 (1969).

61. C.V. Berney, Spectrochim. Acta, 20, 1437 (1964).

62. M.K. Wilson and S.R. Polo, J. Chem. Phys., 20, 1716 (1952).

63. A. Muller, O. Glemser and E. Niecke, Z. Naturforsch., B21, 732 (1966).

64. M. Halmann, Spectrochim. Acta, 16, 407 (1960).